Pleistocene reindeer dental calculus as a source for ancient oral and digestive flora

Authors
Fabian L. Kellner[1,2], Jaelle C. Brealey[1,3], Sarah L. F. Martin[1], Mikkel Winther Pedersen[4], Vebjørn Veiberg[5], Vanessa C. Bieker[1,2], Katerina Guschanski[6,7], Michael D. Martin[1,2]

[1] Department of Natural History, University Museum, Norwegian University of Science and Technology, Trondheim, Norway

[2] Centre for Biodiversity Dynamics, Department of Biology, Norwegian University of Science and Technology, Trondheim, Norway

[3] Department of Terrestrial Biodiversity, Norwegian Institute for Nature Research, Trondheim, Norway
[4] Centre for Ancient Environmental Genomics, Globe Institute, University of Copenhagen, Denmark
[5] Department of Terrestrial Ecology, Norwegian Institute for Nature Research, Trondheim, Norway
[6] Department of Ecology and Genetics, Animal Ecology, Uppsala University, Uppsala, Sweden
[7] School of Biological Sciences, The University of Edinburgh, Edinburgh, United Kingdom

Abstract

Dental calculus forms when the biofilm found on teeth calcifies during an individual's lifetime, simultaneously encasing and preserving microorganisms and biomolecules, including DNA. Dental calculus contains genetic information from the oral microbiome, including potential pathogens, as well as DNA from food sources and a small amount of host DNA. In the case of ruminant animals, regurgitated gut microbes can also be detected. Under favorable conditions, DNA in dental calculus can be preserved for thousands of years and thus presents unique opportunities to study ancient metagenomic material from archaeological remains. Here, we present results from a project aiming to taxonomically characterize the ancient oral metagenome of reindeer (*Rangifer tarandus*) originating from Pleistocene archaeological sites in the Vézère Valley of southern France. This region served as a glacial refugium during the last glacial maximum, but reindeer subsequently became extinct there and are today found only in more northern arctic and boreal regions. We extracted DNA from the surface of 19 ancient reindeer teeth (15,000 – 25,000 years BP) for shotgun metagenomic sequencing and compared these results to microbiomes we obtained from reindeer dental calculus sampled from 45 wild reindeer from both extant and historical populations in Europe. We identified known components of the oral microbiome, and microbes likely originating from the rumen. While putative oral microbiomes differed considerably between ancient and modern samples, we identified six bacterial taxa detected in both ancient and modern samples, all of which are associated with the gastrointestinal tract. As soft tissue is often not preserved in ancient remains, the use of dental calculus of ruminant animals holds a unique opportunity to study both the oral microbiome composition and the microbiome of the digestive tract of extinct populations.

Introduction

Many animals form tightly linked symbiotic relationships with their associated microbial communities (McFall-Ngai 2002). The host and its associated microbes form a holobiont which likely co-evolved over thousands of years (Rosenberg and Zilber-Rosenberg 2018; Scott et al. 2022). Beneficial microbes are involved in many functions vital to the host organism, such as digestion or immune defense, important processes which can not be conclusively understood without studying the microbiome (Lee and Mazmanian 2010; Nieuwdorp et al. 2014; Nikitakis et al. 2017). The microbes colonize a variety of soft tissues, for example the skin, oral cavity and digestive tract of their hosts (Nichols, Peters, and Patterson 2019). The oral microbiome is of special interest since it acts as the direct interface between the host's exterior environment and the host's digestive and respiratory tracts and their resident microbiomes (Moraitou et al. 2022). However, the study of long-term holobiont evolution requires materials that survive *post-mortem* decay and go on to fossilize.

Dental calculus is mineralised dental plaque that continuously calcifies during an animal's lifetime (Key et al. 2017; Jin and Yip 2002). The microbial community composition changes over time as the plaque matures, and early colonizers facilitate the colonization of additional species that come later (Ramberg et al. 2003; Kolenbrander Paul E. et al. 2002). In this process, the DNA of microbes and other materials present in the oral environment are encased and preserved over the host’s lifetime, and sometimes for thousands of years after the host’s death (Mann et al. 2018). This property makes dental calculus an interesting material for the study of host-associated microbiomes and their temporal evolution (Warinner, Speller, and Collins 2015; Modi et al. 2020; Brealey et al. 2020). Since the genomic material stays relatively stable over millennia, this opens new avenues for the research of past microbial communities. For example, ancient dental calculus has been used in primates to track changes in microbiome diversity (Granehäll et al. 2021; Yates et al. 2021) and diet (Ottoni et al. 2019). However, non-primate, non-model-organism studies of oral microbiomes and dental calculus are thus far underrepresented (Brealey et al. 2020; Ozga and Ottoni 2023).

The reindeer (*Rangifer tarandus*, Linnaeus 1758) is an arctic and sub-arctic (Lin et al. 2019), semi-domesticated cervid with circumpolar distribution (Yannic et al. 2018). Reindeer are of commercial and cultural value for humans (Burch 1972; Müller-Wille et al. 2006), but are understudied in comparison to other ruminant livestock species, such as cow (*Bos bovis*), sheep (*Ovis aries)* and goat (*Capra hircus*). As ruminants, reindeer regularly regurgitate their rumen content into their oral cavity for repeated mastication, which introduces members of the digestive tract into the oral environment (Kittelmann et al. 2015; Tapio et al. 2016; Amin et al. 2021) and therefore potentially into dental calculus (Brealey et al. 2020). The microbial community composition of the gut gradually changes from one end of the digestive tract to the other (Michelland et al. 2009; de Oliveira et al. 2013; Frey et al. 2010; Kamenova et al. 2023; Tapio et al. 2016).

However, most of the knowledge outlined above is based on the study of common livestock animals and comparatively little is known about the reindeer microbiome to date. The

community in the oral (Ozga and Ottoni 2023) and rumen (Glendinning et al. 2021; Østbye, Wilson, and Rudi 2016) microbiome can differ substantially between mammalian species, so the assumptions about the reindeer microbiome that we can draw based on other species is severely limited. Previous studies on the rumen microbiome of reindeer found high abundances of methanogenic archaea (Sundset et al. 2009), numerous novel rumen uncultured bacteria (RUGs (Glendinning et al. 2021)), and even 18 metagenome-assembled genomes (MAGs) characterized to the species level (Kamenova et al. 2023), but there remains much to be learned from further research on reindeer-associated microbiomes. Furthermore, historical changes in microbiome composition of reindeer have not been studied at all. Reindeer underwent substantial range fluctuations throughout the Pleistocene and more recently underwent a northward range shift in the Holocene (Flagstad and Røed 2003; Lorenzen et al. 2011; Sommer et al. 2014). Dental calculus provides a unique opportunity to study the ancient oral and rumen microbiomes of ruminants and to learn about the evolution of microbiomes from tissues which are usually inaccessible from the fossil record.

Metagenomics, the sequencing of DNA from all genomes in a mixed sample, allows the characterisation of host, microbial and environmental genetic material from a single sample (Frioux et al. 2020). With the advances in the study of ancient DNA (aDNA), ancient metagenomics has become a more accessible field of study (Warinner et al. 2017). However, ancient metagenomics is not without its challenges (Brealey et al. 2020; Prüfer et al. 2010; Ziesemer et al. 2015; Warinner, Speller, and Collins 2015). Ancient DNA is challenging to work with due to very short DNA fragments and a characteristic damage pattern manifested as cytosine-to-thymine transitions caused by post-mortem processes (Briggs et al. 2007). Due to the small amount of endogenous DNA in ancient samples, they are vulnerable to contamination by vastly more abundant modern DNA during specimen handling and sample processing (Salter et al. 2014; Eisenhofer et al. 2019). Regarding ancient metagenomes, they could be contaminated by residual DNA from the host's environment (Key et al. 2017), a factor especially relevant for archaeological samples (Llamas et al. 2017; Yang and Watt 2005). Lastly, microbial reference databases have strong biases towards microbes of relevant medical or biotechnological significance to human society, which hinders read-based identification (Rinke et al. 2013).

Ancient dental calculus has only relatively recently gained interest as a material for genomic investigation, and these studies have largely focused on ancient humans and primates (Warinner et al. 2014; Warinner, Speller, and Collins 2015; Modi et al. 2020; Yates et al. 2021; Granehäll et al. 2021; Moraitou et al. 2022). There are only a few studies investigating dental calculus of non-human animals. Therefore ancient, non-primate, non-model organism dental calculus research is an interesting and yet understudied field (Brealey et al. 2020, 2021; Ozga and Ottoni 2023). Indeed, (Brealey et al. 2020) is the only study to date to investigate dental calculus of reindeer, their oldest specimen having died 163 years ago in 1861. They found overall lower oral microbiome diversity, with more uncharacterized taxa, than that of other mammals like the brown bears (*Ursus arctos*) and the eastern gorilla (*Gorilla beringei*), and that several typical mammalian oral microbiome members (e.g. *Streptococcus*) are almost entirely absent. Further, they identified reindeer-specific *Methanobrevibacter* related to

rumen-associated species such as *M. ruminantium* and *M. olleyae*, which indicates that some portion of the rumen microbiome is captured in reindeer dental calculus (Brealey et al. 2020).

Here, we used ancient dental calculus material from the teeth of reindeer (*Rangifer tarandus,* Linnaeus, 1758) to generate ancient metagenome-assembled genomes (MAGs), which we used to investigate the potential of paleo-genomic dental material to capture information about the oral microbiomes of prehistoric reindeer. Our aims were to understand how well the diversity of the reindeer oral microbiome has been conserved over the past 30,000 years, and to explore ancient dental calculus as a tool for better understanding mammalian ecology and evolution during the Pleistocene. Among our results are the oldest oral microbiomes from non-primate samples, dating back to 23,009 cal BP. For comparison we additionally generated the first dental calculus metagenomes from contemporary wild reindeer. We hypothesized that due to the role of regurgitation in ruminant digestion, ancient dental calculus would preserve microbes that originated in the gastro-intestinal tracts of animals that died over 23 thousand years ago.

Materials and Methods

Modern reindeer dental calculus sampling

The modern wild reindeer material (see Table 1) used in this study was collected by hunters as part of the Norwegian national monitoring program for cervids, managed by the Norwegian Institute for Nature Research (NINA) on behalf of the Norwegian Environment Agency. The reindeer were hunted from wild populations in Rondane Sør (61.88°N, 9.80°E; *n*=11) and Forollhogna (62.68°N, 10.79°E; *n*=10), two of six monitoring areas for wild reindeer in mainland Norway, during the annual reindeer hunt between August and September 2021. Hunters register information, including kill date, location, and animal sex in a national database (www.hjorteviltregisteret.no). Hunters deliver the pre-cleaned and dried lower mandibles, which are then measured and used to assess age at death at NINA in Trondheim, Norway. Age determination for individuals two years and older was determined based on readings of cementum annuli in decalcified and stained longitudinal sections (Veiberg et al. 2020). To allow easy and non-destructive extraction of the incisors used for age determination, the jaws were boiled for approximately 90 minutes. After boiling, dental calculus samples were collected from one half of an air-dried mandible of each reindeer individual in the wild animal processing room at NINA. During sampling, all surfaces were decontaminated with bleach and then wiped with ultra-pure molecular biology water. A fresh aluminum foil sheet was used as the working surface for each sample. Gloves and scalpel blades were changed between each sample and protective clothing was worn, including one-way lab coats, double gloves taped to the lab coat so that no skin was exposed during sampling, and face masks. Material was collected by scraping off the dental calculus deposits from all teeth in the mandible, including both lingual and buccal sides. In most cases, the majority of the material was collected from molars and premolars, only rarely the incisors were included as well, aiming for ca. 50 mg of material from each individual. Afterwards, samples were stored in microcentrifuge tubes at room temperature for 1 week before being frozen at -20°C until DNA extraction.

Ancient reindeer dental calculus sampling

The ancient reindeer material used in this study consists of 19 museum specimens loaned from the French National Museum of Prehistory (Musée National de Préhistoire, MNP) in Les Eyzies, Dordogne, France (see Table 1). The material was excavated from Cro-Magnon settlement sites situated in rock shelters (French: *abris*), where they were likely transported to from off-site hunting grounds. The archaeological sites are situated in the Vézère Valley in the near vicinity of the museum in Department Dordogne. Five samples were excavated in the early twentieth century by J. A. Le Bel and J. Maury from middle and upper Magdalenien layers from Abri Laugerie-Basse (sample code 'LB', (Maury and Le Bel 1925)). Another 14 samples (sample code 'U') were excavated in the early twentieth century by Denis Peyrony either at Abri de la Madeleine (middle and upper Magdalenien) or Abri Laugerie-Haute Ouest (Solutrean), but the exact records have been lost to time, therefore attribution to the sites remains uncertain. Since archaeological context does not allow for certainty in attributing one or more bones/teeth to one or more reindeer individuals, all samples are lower right-side third molars (M_3) of which a reindeer typically has only one.

All ancient samples were processed at a dedicated paleo-genomics facility at the NTNU University Museum. To remove surface contamination, the teeth were irradiated with UV light for 10 minutes on each side and subsequently decontaminated using EDTA, following the recommendations by (Brealey et al. 2020). 10-20 mg of dental calculus powder was collected by grinding the tooth surface with a Dremel rotary saw equipped with a file head. To avoid outside and cross-contamination, subsampling was conducted inside a laminar flow-hood, which was decontaminated between samples with 5% (v/v) bleach and 70% EtOH. Dental calculus powder was collected using clean aluminum foil, which was exchanged between samples. All ancient samples were carbon-dated at the NTNU University Museum's National Laboratory for Age Determination.

Historical reindeer dental calculus samples data

We complemented our dataset of ancient and modern reindeer dental calculus with previously published short-read data from specimens of six historical reindeer that died between 1856 and 1960 (mainland Norway n = 1, Svalbard n = 3, Greenland n = 1, Unknown n = 1, Table 1) and are stored in the collections of the Swedish Museum of Natural History (Stockholm) (Brealey et al. 2020). One of these samples ("Rt_tooth") was a fragment of reindeer tooth crown which serves as control for tooth surface and external contamination in contrast to authentic dental calculus. The negative blank controls from this study were also downloaded and processed, to account for study-specific laboratory contamination. The sequence data was retrieved from the European Nucleotide Archive (ENA) at EMBL-EBI under accession number PRJEB33363 (https://www.ebi.ac.uk/ena/browser/view/PRJEB33363).

DNA extraction, library building and sequencing

For all samples, all pre-PCR steps were performed in laboratories that are free of PCR products. Ancient samples were processed in separate, dedicated, positively pressurized clean-room facilities, while modern samples were processed in a conventional molecular biology laboratory.

DNA extraction from dental calculus powder was conducted using a protocol especially developed by (Brealey et al. 2020) for non-human, mammalian dental calculus based on an adaptation of the protocol from (Dabney et al. 2013). Each extraction batch was accompanied by negative blank controls containing no sample material, for the subsequent identification of laboratory contaminants. The extracted modern genomic DNA was sheared to a mean fragment length of 350 to 500 bp using a Covaris ME220 focused ultrasonicator. For each sample and the extraction blanks, 20 µL of DNA extract were built into single-stranded libraries, following the *Santa Cruz Reaction* library preparation method (Kapp, Green, and Shapiro 2021). DNA extraction blanks were included, as well as a library blank (no-template control). The optimal number of PCR cycles for each library was determined via qPCR on a QuantStudio3 instrument (ThermoFisher), then each library was amplified using a dual indexing approach (Kircher, Sawyer, and Meyer 2012). The indexing PCR buffer mix consisted of (per sample) 0.8 µL 25 mM dNTPs (final conc. 0.2 mM), 5 U/µL AmpliTaq Gold polymerase (final conc. 0.05 U/µL), 10 uL 10X AmpliTaq Gold buffer (final conc. 1X), 10 µL 25 mM MgCl2 (final conc. 2.5 mM), 0.8 µL 50 mg/mL BSA (final conc. 0.4 mg/mL) and 63.4 µL ultra-pure molecular grade H_2O, 10 µL DNA template and 2 µl of 100 µM dedicated P5 and P7 index each. Based on the qPCR results, in the indexing PCR modern samples were given 10 cycles, modern blanks were given 14 cycles, ancient samples were given 5 to 14 cycles and ancient blanks were given 21 cycles. The indexing PCR settings consisted of a 10 minute hot-start at 95 °C, followed by a sequence of 30 seconds at 95 °C, 60 seconds at 60 °C, and 45 seconds at 72 °C, repeated for the given number of cycles. Final extension lasted for 5 minutes at 72 °C. The PCR product was purified using SeraMag beads in bead:DNA ratio of 9:10 and eluted in 33 µL Qiagen EBT buffer. The amplified libraries were quantified on 4200 TapeStation instrument (Agilent Technologies) using High Sensitivity D1000 ScreenTape. The libraries were then pooled in equimolar concentrations and subsequently subjected to several rounds of PE 150 bp sequencing on the Illumina NovaSeq 6000 platform (Novogene UK).

Sequencing data processing

Sequence data from the pooled libraries were demultiplexed according to their unique dual-index barcode combinations. Read pairs with the default overlap length of ≥ 11 bp were collapsed, residual adapter sequences were removed and reads shorter than 25 bp were discarded with *AdapterRemoval* v2.2.4. Trimmed sequencing reads were mapped against a caribou (*R. t. caribou*) reference genome assembly (Taylor et al. 2019) with the *paleomix* pipeline v1.7 (Schubert et al. 2014) using the 'mem' algorithm of the *Burrows-Wheeler Aligner* (*BWA*) v0.7.16a (H. Li 2013) and no mapping quality (MAPQ) score filtering. We discarded reads that mapped to the caribou reference and extracted unmapped reads with *samtools* v1.12. From these unmapped reads, PCR duplicate reads were removed with *seqkit* v2.3.0. We

then mapped only the collapsed reads against the human nuclear and mitochondrial reference genomes (genbank accession number GCF_000001405) to further remove possible contamination from processing the samples. We chose to only use the overlapping/collapsed reads because we expect the DNA in dental calculus to be fragmented, therefore longer fragments are likely to be modern contamination (see (Brealey et al. 2020)). As before, we discarded reads mapping to the reference and extracted reads with samtools. We considered these leftover reads to be of putative microbial origin (henceforth referred to as 'microbial reads').

Metagenomic analysis

In order to accurately characterize the microbiome at lower taxonomic levels, we generated metagenome-assembled genomes (MAGs) following the *metaWRAP* v1.3.2 pipeline (Uritskiy, DiRuggiero, and Taylor 2018), processing ancient and modern samples separately throughout. First, we assembled the reads into longer contigs. We opted for a co-assembly strategy using *MEGAHIT* v1.2.9 (D. Li et al. 2015), in which reads from multiple samples are assembled together, since this strategy increases the usefulness of very low coverage data. We ran two co-assemblies, one each for all ancient samples (including the downloaded historical metagenomes, 'ancient assembly batch') and all modern samples ('modern assembly batch'), with a minimum contig length of 1000 bp (*--min-contig-len* 1000) and the 'meta-sensitive' preset (*--presets meta-sensitive*). We chose this grouping of samples since historic samples and ancient samples share characteristic *post-mortem* damage patterns that the freshly collected modern samples do not share. Microbial reads from blank control samples were not included in the assemblies, but were mapped back to the assemblies during binning to identify putative laboratory contaminants (see below).

To assess ancient DNA degradation, we utilized *mapDamage2* (Jónsson et al. 2013) to analyze the microbial reads for every ancient and historical sample using the collection of *Anvi'o* contigs acting as reference. In addition, in the case of the six taxa that appeared in both ancient and modern samples, we mapped the ancient microbial reads against the respective MAGs with the *paleomix* v1.7 bioinformatic pipeline (same settings as above), including built-in damage assessment with *mapDamage2* with default settings. We used the *decOM* pipeline (Duitama González et al. 2023) to track the putative sources of the metagenomic reads in our dental calculus. The pipeline was run separately for the ancient and modern sample groups, both times with the default *decOM* source matrix. To account for miscalls caused by aDNA damage we used the method described in (Klapper et al. 2023), which is implemented as part of the *nf-core/mag* pipeline (v2.5.4) (Krakau et al. 2022) within the *nf-core* framework (Ewels et al. 2020). Since the aDNA subworkflow is currently not implemented to work with co-assembly input as of version 2.5.4, we concatenated our input reads into a single file and ran the pipeline in single-assembly mode. Apart from the aDNA subworkflow, all other parts of nf-core/mag were skipped.

We checked for reads mapping to the common Illumina sequencing control, phiX 174, by mapping the microbial reads against the phiX reference genome (RefSeq acc. No.

GCF_000819615.1) with PALEOMIX v1.7 as described above. Since the total number of reads mapping to PhiX in each sample were negligible (min = 0, max = 10, mean = 0.8) we did not remove those reads before further processing.

The assembled contigs were then processed with the *Anvi'o* pipeline (Eren et al. 2021). Open-reading frames within contigs were identified with *Prodigal* (Hyatt et al. 2010). Contigs were then annotated using hidden Markov models (HMMs), searching against *Anvi'o*'s collections of bacterial single-copy genes, as well as KEGG (Kanehisa and Goto 2000) and Pfam (Mistry et al. 2021) functional annotations. *Anvi'o* sample and depth profiles for binning were generated by mapping the original microbial reads from each sample, including blank samples, against all contigs from their respective co-assembly with the *mem* algorithm in *BWA* v0.7.17-r1188, in a manner similar to competitive mapping, where the reads are mapped against a reference concatenated from multiple reference genomes (Feuerborn et al. 2020). The resulting bam files were then further profiled with *anvi-profile* using a minimum contig length of 1000 bp. The resulting sample profiles were hierarchically clustered based on depth profiles into a single merged profile database for downstream analysis with *Anvi'o*.

To ensure high accuracy for taxonomic classification, we binned (i.e. sorting the contigs into likely operational taxonomic units (OTUs)) contigs with three independent, automated metagenomic binning softwares: *Metabat* v2.12.1 (Kang et al. 2014) with default parameters*, Maxbin* v2.0 (Wu, Simmons, and Singer 2016)*,* with default parameters and *Concoct* v1.1.0 *(Alneberg et al. 2014),* with default parameters and number of clusters set to 100, which we chose based on preliminary analysis of the data.

The results of the three binning softwares were refined and dereplicated with *metaWRAP*'s built-in refinement module, using a 50% completion threshold and a 20% redundancy/contamination threshold as calculated by *checkM* (Parks et al. 2015). A Wilcoxon test in *R* (v4.2.3) (R Core Team 2021) was used to test for differences in completion, redundancy and guanine-cytosine (GC) content between the two co-assembly batches. The finished MAGs were then taxonomically classified with the Genome Taxonomy Database (release 207_v2) using the associated Genome Taxonomy Database Toolkit (*gtdb-tk* v2.2.4, (Chaumeil et al. 2019, 2022)).

We then used *dRep* 'compare' (Olm et al. 2017) to find MAGs which were assigned the same taxonomy in the modern and ancient batches. MAGs were considered of identical taxonomy when the primary algorithm (*Mash*, (Ondov et al. 2016)) assigned more than 90% shared average nucleotide identity (ANI) and the secondary clustering algorithm (*ANImf*, (Richter and Rosselló-Móra 2009)) assigned at least 90% shared ANI. If one or both methods yielded lower results than the threshold, we considered the MAGs sufficiently distinct to consider them separate taxa. Summary statistics were computed by *Anvi'o*. In *Anvi'o*, abundance is calculated as the mean coverage of a contig divided by the mean coverage of all contigs in that sample. In addition, *Anvi'o* calculates a detection value, which equals the proportion of nucleotides in any one bin that have at least 1X coverage in a sample. We considered a bin as sufficiently well detected in a sample when the detection value was above 0.3.

The *Anvi'o* summary statistics for detected MAGs in the modern and ancient datasets, including blank controls, were then combined and analyzed in *R* (v4.2.3) (R Core Team 2021) with the *phyloseq* (McMurdie and Holmes 2013)*, decontam* (Davis et al. 2018) and *maaslin2* (Mallick et al. 2021) packages. *Decontam* was used to identify and remove likely laboratory contaminant taxa based on their prevalence in the blank controls, using the default probability threshold of 0.1. After removing contaminants, we log-transformed filtered abundance values and used the *vegan (Blanchet et al. 2022)* package to calculate a matrix of dissimilarity indices (based on Euclidean distance) which was used as input for a principal coordinate analysis (PCoA) with the *ape* package (Paradis and Schliep 2019), as well as to conduct a permutational multivariate analysis of variance (PERMANOVA) using age class (ancient, historical, modern) and number of microbial reads as variables. To explore possible biases between the sampling areas of the modern reindeer populations, we additionally conducted a PERMANOVA using individual age, area and number of microbial reads as variables. We calculated a projected PCA onto the PCoA with *R* code developed by Matthias Grenié (https://gist.github.com/Rekyt/), which itself uses the formula from (Legendre and Legendre 1998). This method is similar to the native method in the *ape* package, but was chosen over the latter for compatibility with *R's ggplot2* package (Wickham, Chang, and Wickham 2016). We investigated whether the modern samples with known ages at death cluster by individual age at death in the PCoA. Further, we used the *vegan* package for an analysis of multivariate homogeneity of group dispersions and a Tukey multiple comparisons of means with a 95% family-wise confidence level. We generated a clustered heatmap of filtered, log-transformed abundances with the *pheatmap R* package (Kolde 2019). For a differential abundance analysis between ancient and modern samples, *Maaslin2* was used with the not-log-transformed abundance values with minimum abundance of 0 and a minimum prevalence of 1%, and the default linear model (LM) method with *Maaslin2's* built-in $\log_2$-transformation but no additional normalization. Blank samples, historical samples and the samples LB003, U035 and U027 were removed from this analysis because they lacked authentic endogenous microbial reads.

Results

Table 1: Overview of samples in this study. Laboratory negative controls (blanks) omitted. “Year of death” in calibrated years before present (BP) for samples of Type “Ancient”, and calendar year (CE) for samples of Type “Historic” and “Modern”. U = Unknown / missing data.

Sample ID	Sex	Age at death [years]	Animal died in [year]	Type	Country	Location	Museum
U001	U	U	21810 – 21260 BP	Ancient	France	Dordogne	Musée National de Préhistoire
U002	U	U	13403 – 13131 BP	Ancient	France	Dordogne	Musée National de Préhistoire
U004	U	U	21831 – 21339 BP	Ancient	France	Dordogne	Musée National de Préhistoire
U005	U	U	21805 – 21211 BP	Ancient	France	Dordogne	Musée National de Préhistoire
U012	U	U	15021 – 14569 BP	Ancient	France	Dordogne	Musée National de Préhistoire
U016	U	U	16047 – 15706 BP	Ancient	France	Dordogne	Musée National de Préhistoire
U018	U	U	23009 – 22390 BP	Ancient	France	Dordogne	Musée National de Préhistoire
U023	U	U	12874 – 12178 BP	Ancient	France	Dordogne	Musée National de Préhistoire
U027	U	U	21822 – 20649 BP	Ancient	France	Dordogne	Musée National de Préhistoire
U031	U	U	22217 – 21723 BP	Ancient	France	Dordogne	Musée National de Préhistoire
U035	U	U	15277 – 14912 BP	Ancient	France	Dordogne	Musée National de Préhistoire
U041	U	U	21755 – 21034 BP	Ancient	France	Dordogne	Musée National de Préhistoire
U048	U	U	21837 – 21234 BP	Ancient	France	Dordogne	Musée National de Préhistoire
U059	U	U	21819 – 21283 BP	Ancient	France	Dordogne	Musée National de Préhistoire
LB003	U	U	U	Ancient	France	Laugerie Basse	Musée National de Préhistoire
LB006	U	U	14830 – 14434 BP	Ancient	France	Laugerie Basse	Musée National de Préhistoire
LB014	U	U	14736 – 14391 BP	Ancient	France	Laugerie Basse	Musée National de Préhistoire

Sample ID	Sex	Age at death [years]	Animal died in [year]	Type	Country	Location	Museum
LB015	U	U	14608 – 14283 BP	Ancient	France	Laugerie Basse	Musée National de Préhistoire
LB017	U	U	13406 – 13084 BP	Ancient	France	Laugerie Basse	Musée National de Préhistoire
R1	M	3	2021	Modern	Norway	Rondane Sør	NTNU Vitenskapsmuseet
R2	M	5	2021	Modern	Norway	Rondane Sør	NTNU Vitenskapsmuseet
R3	M	3	2021	Modern	Norway	Rondane Sør	NTNU Vitenskapsmuseet
R4	M	5	2021	Modern	Norway	Rondane Sør	NTNU Vitenskapsmuseet
R5	F	9	2021	Modern	Norway	Rondane Sør	NTNU Vitenskapsmuseet
R6	F	11	2021	Modern	Norway	Rondane Sør	NTNU Vitenskapsmuseet
R7	M	2	2021	Modern	Norway	Rondane Sør	NTNU Vitenskapsmuseet
R8	F	7	2021	Modern	Norway	Rondane Sør	NTNU Vitenskapsmuseet
R9	F	10	2021	Modern	Norway	Rondane Sør	NTNU Vitenskapsmuseet
R10	F	15	2021	Modern	Norway	Rondane Sør	NTNU Vitenskapsmuseet
R11	M	4	2021	Modern	Norway	Rondane Sør	NTNU Vitenskapsmuseet
F1	M	3	2021	Modern	Norway	Forollhogna	NTNU Vitenskapsmuseet
F2	M	4	2021	Modern	Norway	Forollhogna	NTNU Vitenskapsmuseet
F3	F	3	2021	Modern	Norway	Forollhogna	NTNU Vitenskapsmuseet
F4	M	6	2021	Modern	Norway	Forollhogna	NTNU Vitenskapsmuseet
F5	F	4	2021	Modern	Norway	Forollhogna	NTNU Vitenskapsmuseet
F6	M	8	2021	Modern	Norway	Forollhogna	NTNU Vitenskapsmuseet
F7	M	6	2021	Modern	Norway	Forollhogna	NTNU Vitenskapsmuseet

Sample ID	Sex	Age at death [years]	Animal died in [year]	Type	Country	Location	Museum
F8	M	6	2021	Modern	Norway	Forollhogna	NTNU Vitenskapsmuseet
F9	F	15	2021	Modern	Norway	Forollhogna	NTNU Vitenskapsmuseet
F10	F	4	2021	Modern	Norway	Forollhogna	NTNU Vitenskapsmuseet
Rt1	U	U	1861	Historic	Norway	Spitsbergen	Naturhistoriska riksmuseet
Rt5	U	U	1960	Historic	U	U	Naturhistoriska riksmuseet
Rt7	U	U	1861	Historic	Norway	Spitsbergen	Naturhistoriska riksmuseet
Rt11	M	U	1950	Historic	Norway	Southwest Norway	Naturhistoriska riksmuseet
Rt13	F	U	1899	Historic	Greenland	Northeast Greenland	Naturhistoriska riksmuseet
Rt_tooth	U	U	1958	Historic	Norway	Spitsbergen	Naturhistoriska riksmuseet

MAG generation and authenticity

Our final dataset consisted of 21 modern and 19 ancient reindeer, as well as 6 historical samples from a previously published study (Brealey et al. 2020) (Table 1). The average number of microbial reads was 24,835,136 (min: 11,299,887, max: 38,662,827) for ancient samples, 3,642,306 (min: 47,090, max: 8,820,877) for historical samples, and 8,333,884 (min: 166,985, max: 14,451,312) for modern samples. For the ancient co-assembly batch, our *MEGAHIT* co-assembly yielded 147,775 contigs with a total length of 369,908,798 bp, with an average contig length of 2,503 bp (min = 1,000 bp (controlled by settings), max = 655,378 bp) and a N_{50} of 2,898 bp. For the modern co-assembly batch, our *MEGAHIT* co-assembly yielded 126,891 contigs with a total length of 308,341,285 bp, with an average contig length of 2,429 bp (min = 1,000 bp (controlled by settings), max = 261,408 bp) and a N_{50} of 2,699 bp. The contigs of both datasets were binned into combined 121 distinct MAGs (62 ancient, 59 modern) that met our quality thresholds. Based on prevalence in blank control samples, one contaminant MAG (*Acinetobacter fasciculus*) was removed from the ancient assembly batch and five contaminant MAGs (*Caulobacter*, *Methylobacterium*, *Nevskia, Obscuribacteraceae, Mesorhizobium terrae*) were removed from the modern assembly batch, reducing the total number of MAGs to 115 (see Supp. Table 1). *Acinetobacter fasciculus* is a member of a genus of common ancient sample contaminants (Salter et al. 2014; Eisenhofer et al. 2019) while *Nevskia*, *Caulobacter*, *Methylobacterium* and *Mesorhizobium* have been previously identified as laboratory contaminants (Salter et al. 2014). While bacteria are dominant among the 115 MAGs we assembled, we also identified six species of archaea (Fig. 4).

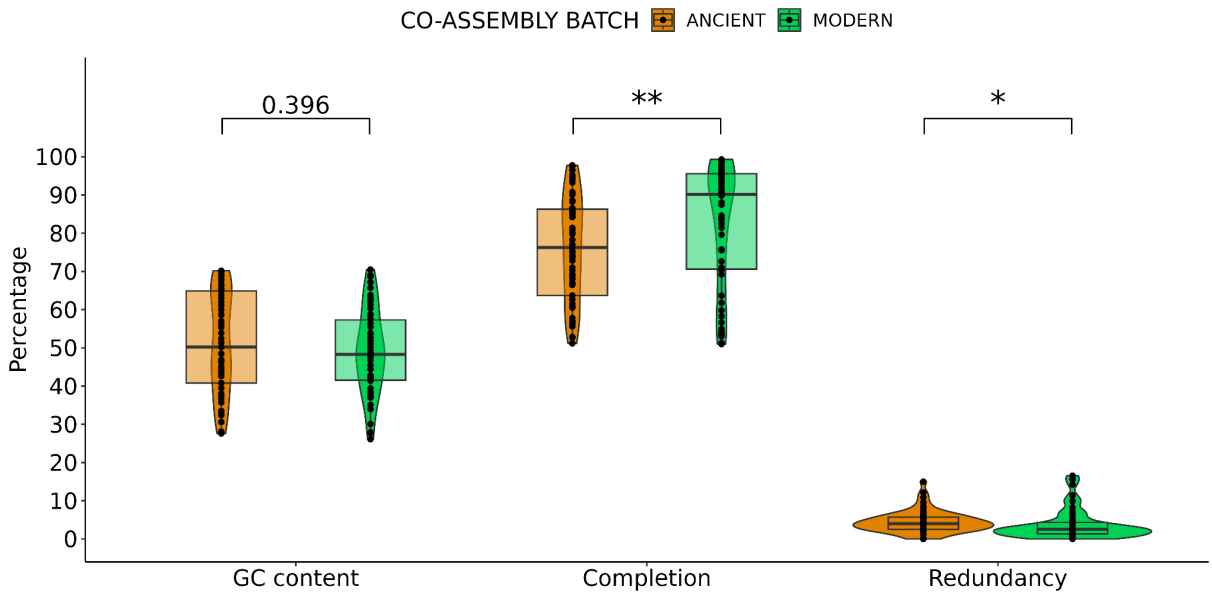

Figure 1: Statistics describing the ancient and modern metagenomic co-assemblies. Relative GC content, completion and redundancy of MAGs are compared between ancient (orange) and modern (green) assembly batches. Each point represents one assembled MAG/bin. Point density at any given percentage is visualized as a violin plot. Boxes represent the 25th percentiles (lower margin), 50th percentiles (median, thick line) and 75th percentiles (upper margin) of the value distribution. Differences in batches were tested with a Wilcoxon test, the significance (p-value) of which is noted in brackets on the top ($p < 0.05$ = *, $p < 0.01$ = **).

Between ancient and modern MAGs, the difference in GC content was not statistically significant ($p = 0.396$, Wilcoxon test), while the differences in completion ($p < 0.01$, Wilcoxon test) and redundancy ($p < 0.05$, Wilcoxon test) were statistically significant (Fig. 1).

To further investigate the authenticity of the remaining MAGs and samples, we used a combination of damage pattern assessment and microbial community analysis. Prior to correcting damage with the *nf-core/mag* pipeline, our ancient and to a lesser degree historical samples show high frequencies of cytosine-to-thymine transitions at the ends of reads, a damage pattern characteristic for aDNA (Fig. 2A). Comparable damage patterns were detected with *mapDamage2* (Fig. 2) and the *PyDamage* (Borry et al. 2021) submodule built into the *nf-core/mag* pipeline's aDNA workflow (Supp. Fig. 5). Microbial reads from the ancient samples LB003 and U035 show unusually low levels of aDNA damage given their age (Fig. 2A, Supp. Fig. 4). These samples group with historical samples and blanks in the PCoA (Fig. 6). Furthermore, these samples also show a microbial community that is different to other ancient samples, with U035 being dominated by taxon *WHSY01 sp*. and none of the top 20 taxa being present in LB003 (Fig. 4). At the MAG level, six MAGs that were present in both ancient and modern samples show high degrees of typical aDNA damage in the ancient samples (Fig. 2B).

The extraction blanks accompanying the modern sample batches have high abundances of a species in the genus *Peptidophaga*, which also occurs in relatively high abundance in most modern samples. The blanks might have been cross-contaminated by the samples; however, since we can not safely rule out that this taxon originates from a different source, we consider it contamination. *Pseudomonas lundensis (Molin, Ternstrom, and Ursing 1986)*, which is found in high abundance in the tooth surface control sample (Rt_tooth) from (Brealey et al. 2020), is very likely a contaminant as well, since it is commonly associated with spoiled meat, i.e. animal carcasses (Molin, Ternstrom, and Ursing 1986; Molin and Ternstrom 1986). These taxa were not excluded from statistical analysis, but were excluded from interpretation of results.

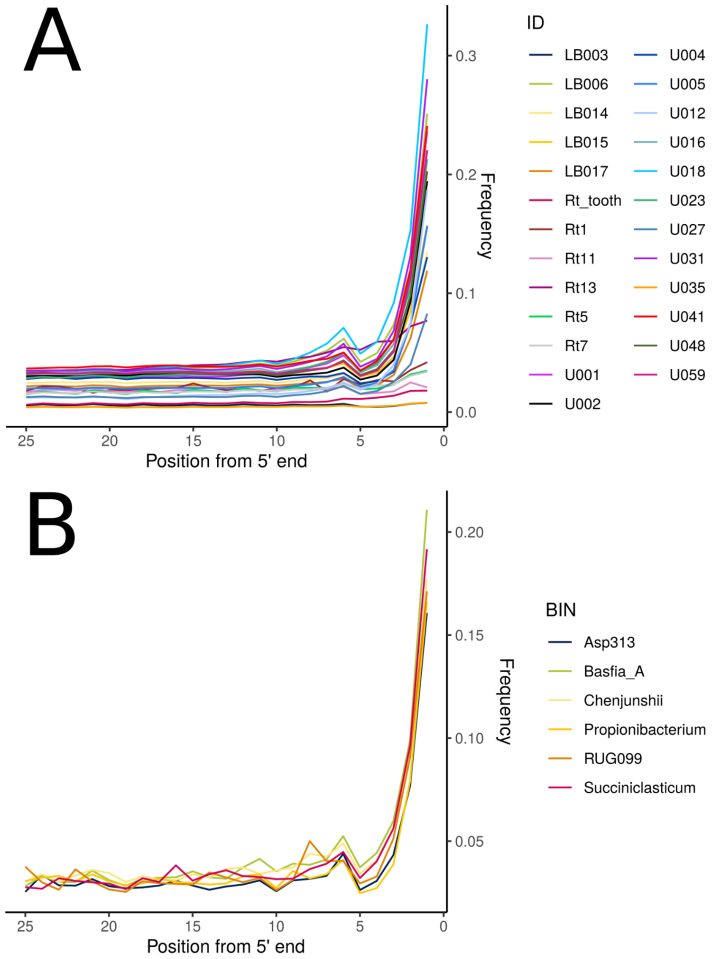

Figure 2: Ancient DNA damage patterns. Frequency of cytosine-to-thymine-transitions on the 5'-end of microbial reads have been calculated with *mapDamage2* (Jónsson et al. 2013). **A)** Ancient DNA damage in ancient and historical samples, based on assembled microbial contigs. **B)** DNA damage patterns in ancient samples for six bins identified in both ancient/historical and modern dental calculus samples.

We used *decOM* with the default database of possible sources (Supp. Fig. 3). The majority of the reads were classified as 'unknown'. Only a small fraction of reads were classified as originating from human skin in the ancient and modern data set, and the modern data set contains only miniscule amounts of reads originating from soil; the amount of soil-originating reads is comparatively larger in the ancient samples. The relative amount of skin contamination is higher in the blanks and some of the historic samples. The modern samples contain a comparatively higher fraction of oral reads than the ancient samples. The oral reads in both datasets are evenly split between ancient oral and modern oral sources.

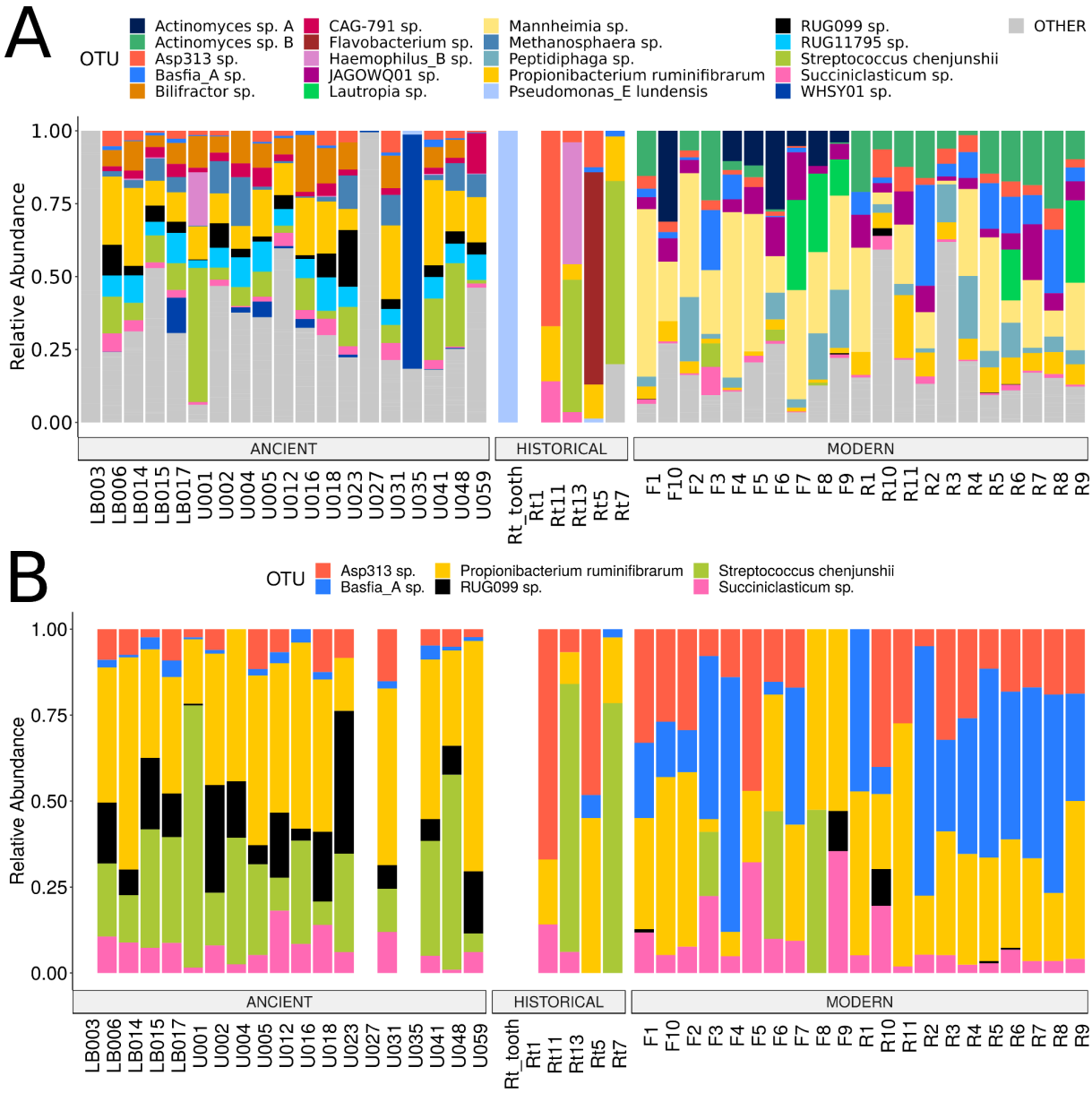

Figure 3: Relative abundance of selected taxa in reindeer dental calculus samples. A: Top 20 most abundant taxa across all samples. All other taxa are collected in 'other' **B:** Only taxa present in both ancient/historical and modern samples. OTU names show the lowest-level assigned taxonomy (genus and/or species). Abundance is corrected for detection threshold (considering samples to be 0 abundance if under detection limit).

Microbial community comparison between sampled datasets

In general, we observe high differentiation by age class (ancient / historical / modern), with most taxa being found only in either the modern, ancient or historical samples (Fig. 3, Fig. 4). In ancient samples, we identified two archaeal species in the genus *Methanobrevibacter* as well as two species in the genus *Methanosphaera* (Fig. 4). These taxa are absent from modern samples. The only species of archaea identified in modern samples was from genus

Methanomethylophilus, which in turn is absent from ancient samples (Fig. 4). In the PCoA, samples cluster distinctively into an ancient cluster, a modern cluster, and a third cluster containing blanks and historical samples, as well as the three ancient samples U027, U035 and LB003 (Fig. 6). This third cluster is weakly sub-clustered into samples with adequate MAG detection (Rt5, Rt7, Rt11 and Rt13) and those without (U027, U035, LB003, Blanks, Rt_tooth, Fig. 6). Modern samples show weak clustering by sampling location (Rondane Sør and Forollhogna); however, when subsetting the modern samples by themselves this trend becomes more evident (Supp. Fig 2). The ancient and modern clusters are separated along PCo1 (Fig. 6). The third cluster sits intermediately between ancient and modern along PCo1, but is about equidistantly removed from both of them along PCo2 (Fig. 6). The biplot shows that the separation of modern and ancient samples on PCo1 is chiefly driven by the taxa which are exclusively present in the corresponding samples, while taxa present in both ancient and modern samples are driving the separation of these samples along PCo2 (Fig. 6). The subclusters of the third cluster are driven mainly by *Pseudomonas lundensis* and to a lesser degree by *WHSY01*. The modern samples with known ages at death did not cluster by age at death (Supp. Fig. 1 & 2), instead grouping by sampling area.

According to the PERMANOVA, the samples are significantly different due to age class (R^2 = 0.200, $p < 0.001$) and only insignificantly different due to the number of microbial reads (R^2 = 0.019, $p = 0.184$) when using these variables together. However, when investigating the effect of these variables independently, both effects increase in strength (age class: R^2 = 0.431, $p < 0.001$; microbial reads: R^2 = 0.249, $p < 0.001$). Focusing on the modern co-assembly batch by itself, samples differ significantly due to sampling area (R^2 = 0.156, $p < 0.001$) and weakly significantly due to individual age at death (R^2 = 0.085, $p < 0.05$) but insignificantly due to the number of microbial reads (R^2 = 0.059, $p = 0.096$). This trend does not change significantly when looking at the variables independently (area: R^2 = 0.168, $p < 0.001$; age: R^2 = 0.087, $p < 0.05$; microbial reads: R^2 = 0.068, $p = 0.113$). The dispersion (average distance to median) was 9.168 for ancient samples, 8.568 for modern samples and 5.525 for historical samples. While modern samples are slightly more clustered than ancient samples, the difference is insignificant (Tukey-test, adjusted $p = 0.717$ [modern / ancient]). Historical samples are weakly, but significantly more clustered than modern samples (Tukey-test, adjusted $p < 0.05$ [modern / historic]), and significantly more clustered than ancient samples (Tukey-test, adjusted $p < 0.05$ [ancient / historic]).
When compared to the 76 MAGs assembled in (Kamenova et al. 2023) which were sampled from the rumen, small intestine and colon of Svalbard reindeer, we were unable to detect any of their 18 species-level MAGs among our own. Furthermore, only the genera *Bacteroides, Prevotella* and *Methanobrevibacter* could be identified in both our study here and (Kamenova et al. 2023).

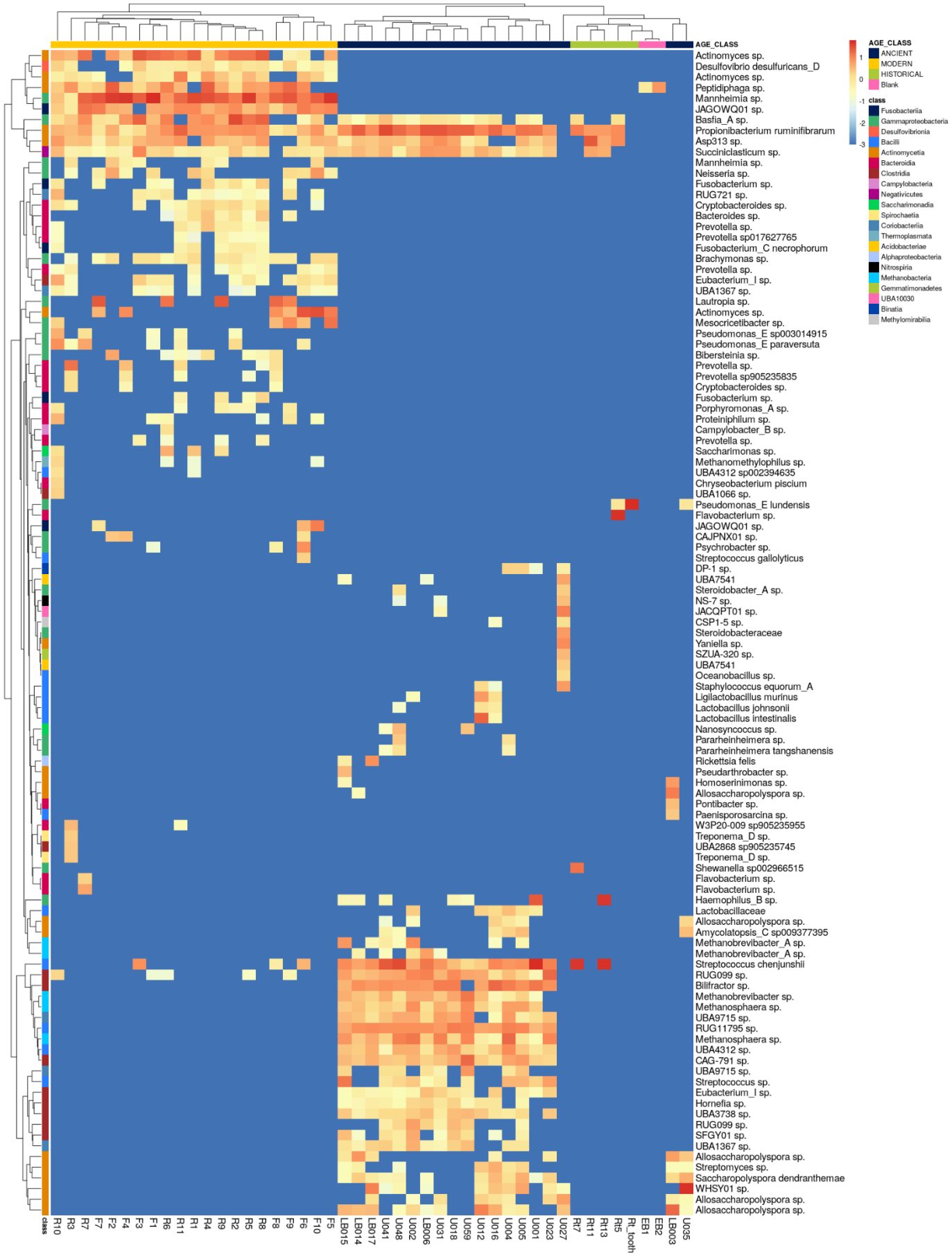
AGE_CLASS
ANCIENT
MODERN
HISTORICAL
Blank
class
Fusobacteriia
Gammaproteobacteria
Desulfovibrionia
Bacilli
Actinomycetia
Bacteroidia
Clostridia
Campylobacteria
Negativicutes
Saccharimonadia
Spirochaetia
Coriobacteriia
Thermoplasmata
Acidobacteriae
Alphaproteobacteria
Nitrospiria
Methanobacteria
Gemmatimonadetes
UBA10030
Binatia
Methylomirabilia
1
0
-1
-2
-3
Actinomyces sp.
Desulfovibrio desulfuricans_D
Actinomyces sp.
Peptidiphaga sp.
Mannheimia sp.
JAGOWQ01 sp.
Basfia_A sp.
Propionibacterium ruminifibrarum
Asp313 sp.
Succiniclasticum sp.
Mannheimia sp.
Neisseria sp.
Fusobacterium sp.
RUG721 sp.
Cryptobacteroides sp.
Bacteroides sp.
Prevotella sp.
Prevotella sp017627765
Fusobacterium_C necrophorum
Brachymonas sp.
Prevotella sp.
Eubacterium_I sp.
UBA1367 sp.
Lautropia sp.
Actinomyces sp.
Mesocricetibacter sp.
Pseudomonas_E sp003014915
Pseudomonas_E paraversuta
Bibersteinia sp.
Prevotella sp.
Prevotella sp905235835
Cryptobacteroides sp.
Fusobacterium sp.
Porphyromonas_A sp.
Proteiniphilum sp.
Campylobacter_B sp.
Prevotella sp.
Saccharimonas sp.
Methanomethylophilus sp.
UBA4312 sp002394635
Chryseobacterium piscium
UBA1066 sp.
Pseudomonas_E lundensis
Flavobacterium sp.
JAGOWQ01 sp.
CAJPNX01 sp.
Psychrobacter sp.
Streptococcus gallolyticus
DP-1 sp.
UBA7541
Steroidobacter_A sp.
NS-7 sp.
JACQPT01 sp.
CSP1-5 sp.
Steroidobacteraceae
Yaniella sp.
SZUA-320 sp.
UBA7541
Oceanobacillus sp.
Staphylococcus equorum_A
Ligilactobacillus murinus
Lactobacillus johnsonii
Lactobacillus intestinalis
Nanosyncoccus sp.
Pararheinheimera sp.
Pararheinheimera tangshanensis
Rickettsia felis
Pseudarthrobacter sp.
Homoserinimonas sp.
Allosaccharopolyspora sp.
Pontibacter sp.
Paenisporosarcina sp.
W3P20-009 sp905235955
Treponema_D sp.
UBA2868 sp905235745
Treponema_D sp.
Shewanella sp002966515
Flavobacterium sp.
Flavobacterium sp.
Haemophilus_B sp.
Lactobacillaceae
Allosaccharopolyspora sp.
Amycolatopsis_C sp009377395
Methanobrevibacter_A sp.
Methanobrevibacter_A sp.
Streptococcus chenjunshii
RUG099 sp.
Bilifractor sp.
Methanobrevibacter sp.
Methanosphaera sp.
UBA9715 sp.
RUG11795 sp.
Methanosphaera sp.
UBA4312 sp.
CAG-791 sp.
UBA9715 sp.
Streptococcus sp.
Eubacterium_I sp.
Hornefia sp.
UBA3738 sp.
RUG099 sp.
SFGY01 sp.
UBA1367 sp.
Allosaccharopolyspora sp.
Streptomyces sp.
Saccharopolyspora dendranthemae
WHSY01 sp.
Allosaccharopolyspora sp.
Allosaccharopolyspora sp.
class
R10
R3
R7
F7
F2
F4
F3
F1
R6
R11
R1
R4
R9
R2
R5
R8
F8
F9
F6
F10
F5
LB015
LB014
LB017
U041
U048
U002
LB006
U031
U018
U059
U012
U016
U004
U005
U001
U023
U027
Rt7
Rt11
Rt13
Rt5
Rt_tooth
EB1
EB2
LB003
U035

Figure 4: Heatmap of the abundance of the 114 MAGs in each sample. Columns are samples, rows are MAGs. Both MAGs and samples have been hierarchically clustered by abundance. Abundance is corrected for detection threshold (considering samples to be 0 abundance if under detection limit.) Abundance values were log-transformed, with a pseudo-count of 0.001 for 0 abundance values (i.e. -3 after log-transformation). MAGs are labeled by their lowest-level taxonomic classification and are annotated by class-level taxonomy. Samples with no detection of any MAG after filtering are excluded from the heatmap (Rt1 and most of the blanks).

Taxa overlapping temporal datasets

Among the 115 putatively non-contaminant MAGs, we identified six that are present in all age classes, and therein were present in almost all samples (Fig. 3). However, none of these taxa were detected in four samples (U027, U035, Rt_tooth, Rt1). These six taxa are *Propionibacterium ruminifibrarum*, Rumen uncultured bacterium 99 (*RUG099 sp.*), *Basfia_A sp., Succinclasticum sp.*, *Streptococcus chenjunshii* and *Asp313 sp.* All of these taxa were first isolated from non-reindeer ruminants, specifically their gastro-intestinal-tracts or feces. Ancient microbial reads mapping to these MAGs show high degrees of typical ancient DNA damage (Fig. 2B).

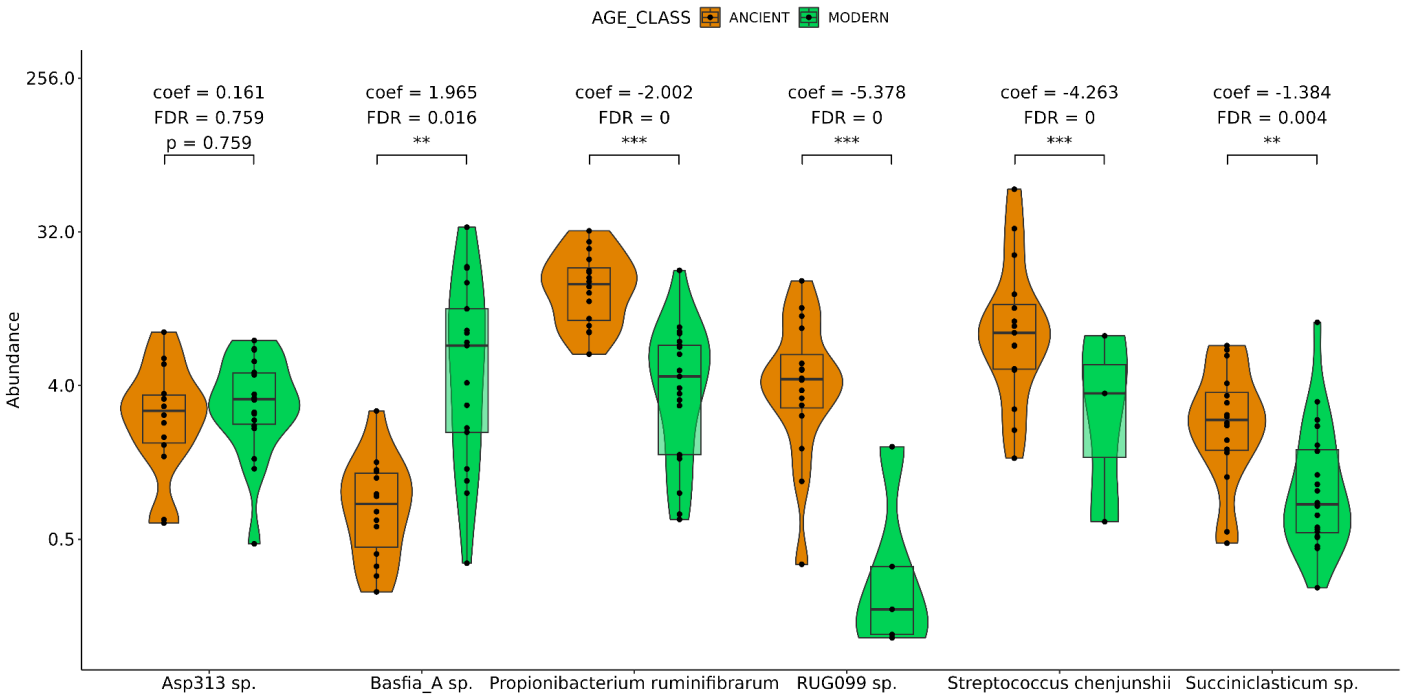

Figure 5: Differential abundance analysis with Maaslin2 (Mallick et al. 2021)**.** Filtered (detection > 0.3) abundance is compared between six taxa present in both ancient (orange) and modern (green) samples. The scale is log2 transformed, which is the default log transformation performed by Maaslin2. Each point represents one sample. Samples in which the taxon is not present are omitted. Point density at any given abundance value is visualized as a violin plot. Boxes represent the 25th percentiles (lower margin), 50th percentiles (median, thick line) and 75th percentiles (upper margin) of the value distribution. Maaslin2 metrics (coefficient (coef), p-value (p), false discovery rate (FDR)) are noted in brackets on the top. Metrics are rounded to three decimal points ($p < 0.01$ = **, $p < 0.001$ = ***).

To further investigate differences between ancient and modern communities, differential abundance analysis was performed with *Maaslin2* (Mallick et al. 2021). For this analysis, we excluded blanks, historical samples (due to the low sample size) and the three ancient samples with outlying/different communities and low signs of ancient DNA damage (U027, U035 and LB003). The analysis yielded 56 significant taxa (FDR < 0.05), 50 of which are bins present only in either ancient or modern samples but not in both (Supp. Table 2). *Asp313 sp.* is present in both datasets, but the *Maaslin2* results were not significant (false discovery rate (FDR) = 0.759, FIg. 5). The other five taxa that are present in both modern and ancient samples have significantly different abundances in the age groups (Fig. 5, Supp. Table 2). *Propionibacterium ruminifibrarum* (FDR = 0, coefficient = -2.002, p < 0.001), *RUG099 sp*. (FDR = 0, coefficient = -5.378, p < 0.001), *Succiniclasticum sp*. (FRD = 0.004, coefficient = -1.384, p = 0.01), *S. chenjunshii* (FDR = 0, coefficient = -4.263, p < 0.001) are more abundant in ancient samples, *Basfia_A sp*. (FDR = 0.016, coefficient = 1.965, p < 0.01) is more abundant in modern samples and *Asp313 sp.* (FDR = 0.759, coefficient = 0.161, p = 0.759) is about equally abundant in both datasets (Fig. 5).

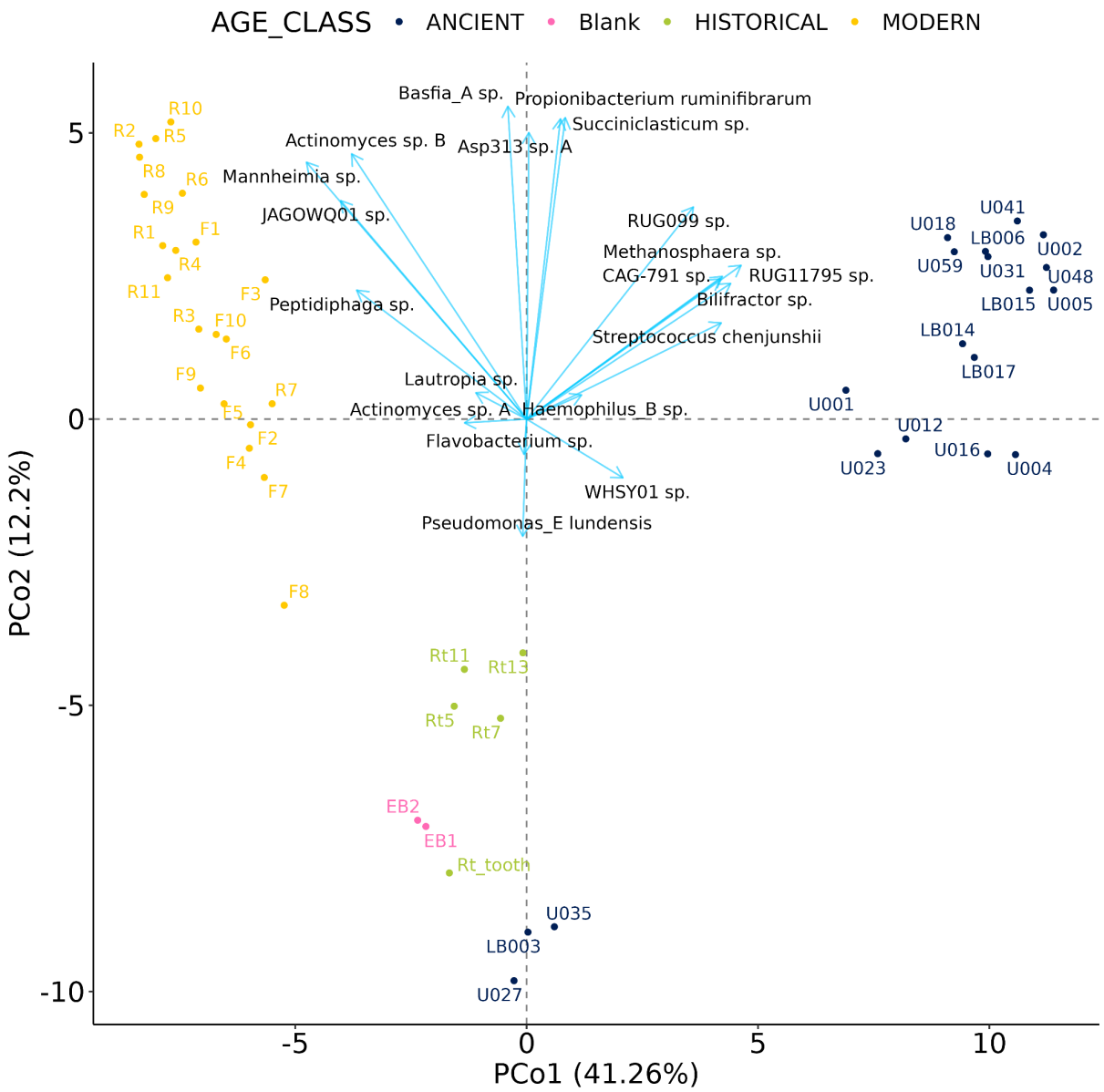

Figure 6: PCoA biplot of the relationship between taxon abundance and samples. Samples are divided into ancient, modern, historical and laboratory blank/control samples. Abundance is corrected for detection threshold (considering samples to be 0 abundance if under detection limit.) Abundance values were log-transformed, with a pseudo-count of 0.001 for 0 abundance values (i.e. -3 after log-transformation). Samples with abundance equal to 0 are omitted. Samples are labeled in the color of their respective age class. The PCoA is overlaid with a projected principal components analysis (PCA) showing the direction of influence of the top 20 most abundant taxa on the distribution (blue arrows). Arrows are labeled with taxon names in black. Arrow lengths have been scaled arbitrarily (but relatively) to increase visibility.

Discussion

Here, we characterized the oral microbiome of both contemporary and prehistoric reindeer. We showed that dental calculus is a suitable source material for the recovery of both oral and gut microbiota in reindeer. While we observe a turnover in microbial community membership and composition between archaeological and fresh material (Fig. 3, 4 & 5), parts of the gut microbiome appear to be remarkably stable throughout time and space (Fig. 3). These six taxa identified in both the ancient and modern oral microbiome (*Propionibacterium ruminifibrarum*, Rumen uncultured bacterium 99 (*RUG099 sp.*), *Basfia_A sp., Succinclasticum sp.*, *Streptococcus chenjunshii* and *Asp313 sp.*) all have putative roles in the reindeer gastro-intestinal-tract.

Identification of contamination and investigation of sample authenticity

One of the most important challenges when working with ancient DNA is the identification of external contamination and discriminating it from authentic endogenous DNA sequences (Eisenhofer et al. 2019; Salter et al. 2014). We identified more laboratory contaminant taxa from blank samples in the modern compared to the ancient dataset. The discrepancy between the number and identity of contaminant species could be explained by the much stricter contamination controls in our ancient DNA facilities in comparison with the museum collections. Another explanation is that modern microbial contaminant reads in the ancient samples would be much longer than authentic ancient reads, and therefore discarded after collapsing of paired end reads. In modern samples, reads were sheared to uniform length, therefore reads from contaminant sources would not be filtered out based on size alone.
We also used damage patterns to assess whether MAGs were putatively authentic dental calculus microbes or modern contaminants, and to identify ancient samples with low levels of authentic ancient DNA. On the MAG level, MAGs that were present in both ancient and modern samples show high degrees of typical DNA damage in the ancient samples (Fig. 2B), suggesting that the presence of these taxa was not caused by contamination of ancient samples with modern DNA. To account for aDNA damage and interpret our results with greater confidence, we used the ancient DNA workflow implemented in *nf-core/mag* (Krakau et al. 2022) to assess and correct aDNA damage, therefore reducing the risk errors further downstream in the analysis.

As should be expected, since the default *decOM* database we used to track read sources is based on human data, the majority of the analyzed reads were classified as ‘unknown’. We assume that this fraction represents the targets of this study, which are the reindeer, reindeer associated-gut microbiome and plant sources, which a human-based database would not contain. In our samples, human skin as source accounts for only a small fraction of reads in the ancient and modern data set, which gives us confidence that we were largely successful in surface decontamination and avoiding additional contamination of our samples during laboratory work. Ancient samples contain a larger fraction of reads sourced from soil, likely reflecting the fact the samples spent thousands of years in soil before being excavated. Conversely, the higher amount of oral reads in the modern samples might be owed to those samples' lack of degradation. Interestingly, in all samples the ratio of ancient oral reads to modern oral reads is

nearly 1:1. It is possible that *decOM* can not clearly differentiate ancient and modern oral taxa, possibly due to taxonomic overlap between temporal datasets.

On the sample level, U035 and LB003 lacked ancient DNA damage patterns, and U035, LB003 and U027 lacked the characteristic dental calculus microbial signatures observed in the other ancient samples. Interestingly, sample U035 was dominated by *WHSY01*. This taxon is a recently discovered bacterial strain of order *Pseudonocardiaceae*, which colonizes fossil remains and was first recovered from DNA sequenced from fossilized bones of a *Centrosaurus* dinosaur (Saitta et al. 2019; Liang et al. 2020). This taxon seems to be a member of a more general microbial community of post-mortem bone colonizers involved in taphonomic processes (Liang et al. 2020). We also found *WHSY01* in lower abundance in a few other ancient samples (Fig. 4). Based on these results, we conclude that no authentic dental calculus microbes were retrieved from samples U035, LB003 *and U027* and that their microbial community is likely of modern origin and/or *post-mortem* contamination. Furthermore, we lack a ^{14}C age for sample LB003 and so cannot confirm its precise age, though it is from the same archaeological assemblage as other LB code samples. We therefore disregard these three samples when discussing the rest of the results.

Compositional differences between ancient and modern reindeer oral microbiomes

The difference in the oral microbiome composition between ancient and modern samples may be explained by several factors. Firstly, the differences in relative abundance of taxa between ancient and modern samples could be explained by preservation bias. The detection of microbial taxa could be skewed due to *post-mortem* decay, which at the same time causes the degradation of authentic microbial DNA as well as colonization by contaminant microbes (Ziesemer et al. 2015). Species with higher GC content (and therefore higher DNA stability) could be better preserved and more stable over time (Mann et al. 2018). While we do indeed observe slightly higher GC content in MAGs assembled from ancient and historical samples compared to those assembled from modern samples, the difference is not statistically significant. Differences in genomic GC content therefore cannot explain the differences in relative abundance of microbes in our samples. Secondly, the large differences in microbial composition could be explained by the range shift of the reindeer from southwestern France to more northerly latitudes over the millenia, and/or different foraging behavior and diet in the two populations (Salgado-Flores et al. 2016; Moraitou et al. 2022). For example, the relative lichen consumption of reindeer was varying due to varying climatic conditions and/or behavioral plasticity throughout the Pleistocene (Britton et al. 2023). Such differences in diet could be investigated with genomic material from dietary components preserved within the dental calculus or coprolites. While our samples did indeed contain a sizable fraction of reads that were assigned to kingdom Plantae in preliminary analysis (data not shown), challenges with dietary analyses from dental calculus, such as low eukaryotic read count, incomplete reference databases and imprecise taxonomic assignment (Mann et al. 2023) necessitate additional research in the future. Thirdly, given the increasingly well understood role of animal host genotype in modulating the gut microbial community (Ryu and Davenport 2022), genetic differences between this study's reindeer populations could in part drive the large differences in microbial composition in our ancient and modern datasets. Lastly, the rising use of antibiotics in

human and livestock medicine and the unwitting spread of antibiotics into the environment could have had a lasting impact on which microbes associate with extant wild animals (Brealey et al. 2021; Karkman, Pärnänen, and Larsson 2019; Bengtsson-Palme, Kristiansson, and Larsson 2018), with clear potential implications for influencing temporal changes in host-associated microbial communities.

Dental calculus can be used to identify modern and ancient rumen microbes

Although we detected major differences between sample age classes, there are six microbial taxa (*Propionibacterium ruminifibrarum,* Rumen uncultured bacterium 099 (*RUG099 sp.*)*, Basfia_A sp., Succinclasticum sp., Streptococcus chenjunshii* and *Asp313 sp.*) that were identified in a majority of samples from both groups, irrespective of age. All six of these taxa are in some way associated with the ruminant gastrointestinal tract. Since they have been previously found in other ruminant host species, it is likely that these taxa, or closely related strains, have a conserved function in the reindeer. That these are the only taxa we find in common across time and space could mean they are important, highly conserved members of the microbiome. A future comparative pangenomics analysis of our study MAGs with strains from other ruminants might test this hypothesis. Since these taxa are found in both ancient and modern dental calculus, we suggest that these six taxa are not environmental contamination but indeed are true members of the reindeer oral and rumen microbiome. Further analysis would be required to confirm this via, for example, an approach in which the dental calculus, oral cavity, rumen and feces are sampled simultaneously from the same animal.

The six taxa of interest are variably well understood, but in every case, each taxon or a closely related strain has been isolated before from ruminant gastro-intestinal tracts or connected systems such as feces, though not the mouth or teeth. *Propionibacterium ruminifibrarum (Vaidya et al. 2019)* is a described, cultured, gram-positive species which was first isolated from the rumen of a dairy cow. In the rumen, *P. ruminifibrarum* ferments propionate and a range of other carbohydrates and amino-acids from plant-fiber material, which are useful substrates for the host (Vaidya et al. 2019). *RUG099 sp.* is an uncultured bacterium from the order Peptostreptococcales*,* MAGs of which have been assembled from reads obtained from cow rumina (Stewart et al. 2018)*. Basfia_A sp.* is a member of the family Pasteurellaceae. *Basfia* and its type species *Basfia succiniproducens* were first isolated and described from cow rumina, where they anaerobically produce succinic acid from glucose (Kuhnert et al. 2010). The type species of genus *Succinclasticum* is *Succiniclasticum ruminis* (van Gylswyk 1995), which was first isolated from cow rumina. There, this bacterium converts succinate to propionate. Other unclassified species or strains in this genus have been found in cattle (Gharechahi et al. 2021) as well as other ruminants, including reindeer (Glendinning et al. 2021). *Streptococcus chenjunshii (Tian et al. 2019)* was first isolated from feces of Tibetan antelope (*Pantholops hodgsonii*), which suggests an association with the gut microbiome. Tibetan antelope is a bovid from the alpine grasslands of Tibet (Wei et al. 2023), not unlike the tundra habitat suitable for reindeer. Tibetan antelope nematode gut parasites *Trichostrongylus*, *Marshallagia* and *Nematodirus spp.* have also been found in Svalbard reindeer (*R. t. platyrhynchus*) (Cao, Foggin, and Zhao 2022; Stien et al. 2002), suggesting similarities between the gastrointestinal tract of these two species. *Asp313 sp*. is a member of the family Actinomycetaceae which has been

isolated from tibetan antelope (BioSample: SAMN08967870) and goat (*Capra hircus*) feces (BioSample: SAMN11294320, (Peng et al. 2021)).

There are still intra-population differences between samples from different individual reindeer, which could be explained by the previously discussed factors in addition to others, such as individual age at death. Since dental calculus forms continuously over the entire lifetime of an individual, its microbial community is also individual- and age-dependent (Utter, Mark Welch, and Borisy 2016). We tested the dispersion of clusters with a PERMANOVA and found that it is similar in ancient and modern samples, which indicates that both groups have similar levels of individual variation. However, as we are not able to identify the age at death of the ancient individuals, we cannot test whether the differences between ancient and modern samples here are due to the effect of age. While we do not know exactly how the ancient reindeer in this study were selected for killing and transport from the kill site to the site of consumption by their prehistoric human hunters, research on prehistoric humans in France (Kuntz and Costamagno 2011; Boyle 1993) and Neanderthals in Germany (Gaudzinski and Roebroeks 2000) and France (Niven et al. 2012) suggests that adult reindeer were preferentially hunted. The modern samples, for which we know the age at death, did not cluster according to their age at death in the PCoA, suggesting that age plays no major role in differences we observe.

The six taxa overlapping temporal data sets are on average more abundant in the ancient samples than in the modern samples. One possible explanation for this difference is that since the oral microbiome is more directly interacting with the environment of the host, it is more strongly affected by changes in the environment, such as changes in diet, climate, or increase of artificial antibiotics in the environment (Moraitou et al. 2022; Brealey et al. 2021). Our analysis of the microbiomes of the two wild modern populations shows that microbiome differentiation between the populations correlates with population affiliation. This could be explained by the differing ancestry of the populations, one of which descends from domesticated reindeer, while the other population has always been wild. Since the populations are geographically separated, differences in the microbiome could also be driven by habitat, which would suggest that the microbiome is sensitive to environmental conditions. Such a sensitivity suggests that ecological factors play a major role in shaping the reindeer oral microbiome (Moraitou et al. 2022; Brealey et al. 2021). Because we are able to attest the strong differences between two contemporaneous populations to ecology, it would be expected that we can attest the differences between the modern populations and ancient populations to the same factors.

Rumen-associated prokaryotic and eukaryotic microbes were also identified in the original analysis of the historical samples by (Brealey et al. 2020), which did not utilize MAGs. However, the authors demonstrated that authentic MAGs can be recovered from non-model animal dental calculus and suggested the more extensive use of MAGs to improve the future analysis of ancient reindeer dental calculus. Here, we were successful in recovering reindeer oral and rumen bacteria by assembling MAGs from a wider variety of samples, further revealing the usefulness of metagenome-assembled genomes. None of the six rumen microbial taxa, which are shared between ancient and modern samples, have been previously reported as members of reindeer microbiomes (Pope et al. 2012; Zielińska et al. 2016; Sundset et al. 2009;

Salgado-Flores et al. 2016). Conversely, taxa in the family *Ruminococcaceae*, which was reported as highly abundant in previous studies (Zielińska et al. 2016; Salgado-Flores et al. 2016; Pope et al. 2012), are completely absent from our MAG assembly results (see Supplementary Table 1). One important reason for this discrepancy may be that these previous studies did not employ MAGs assembled from whole-genome shotgun-sequencing data as done here, but instead used 16S rRNA amplicon sequencing. Both MAGs and 16S rRNA can be biased toward detecting certain taxa in ancient metagenomic datasets (Velsko et al. 2018; Ziesemer et al. 2015; Warinner et al. 2017), thus neither perfectly detect the entire microbiome. Furthermore, previous studies were based on different source material, mainly feces, which might be a less accurate proxy for the rumen microbiome (Tapio et al. 2016). A final explanation for the inconsistencies of our results with previous reindeer microbiome studies could be that feces are food matter passed through multiple stomachs and are therefore altered by local microbiomes, while rumen content is directly regurgitated into the mouth.

Conclusion and future directions

Our work demonstrates that with advanced techniques in ancient DNA sequencing and metagenome assembly, it is possible to retrieve microbial genomes from mammal dental calculus samples surpassing 20 ka BP in age. Our study suggests that certain rumen-associated taxa have been more temporally stable than the oral microbiome, therefore we highlight the potential for utilizing dental calculus to not only study the ecology and evolution of the oral microbiome, but also the ruminant gastrointestinal tract.

This work sets the stage for future research of reindeer holobiont ecology and evolution. Future studies could dramatically expand both spatial and temporal range and density of sampling. *Rangifer tarandus* is subdivided into numerous subspecies that occupy varying habitat types and dispersal ranges throughout the northern Holarctic realm. We hypothesize that various reindeer subspecies could differ in the composition of their microbiomes, as has been observed in other mammalian species (Moraitou et al. 2022). Furthermore, by sampling more reindeer dental calculus from ancient samples from additional former habitats and time frames, one could trace the evolution of the microbiome through time and space and link it to past reindeer range expansions and contractions caused by ice sheet retractions and expansions. However, better understanding of the contemporary reindeer microbiome is needed to give context to past microbial changes. Research on the microbiomes of reindeer and other ruminants could therefore be further advanced by an integrative approach combining dental calculus, buccal swabs, direct gut sampling, bolus and feces. Such approaches would further our understanding of colonization dynamics among the microbial niches of the gut, rumen and oral cavity.

Dental calculus also contains plant DNA from putative food plants of reindeer. This could be used to better understand reindeer diet on a spatiotemporal level throughout the Pleistocene and might even be suitable as a proxy for the distribution of certain plant species (Brealey et al. 2020). If combined with records of past vegetation distributions (e.g. from the pollen record), we could learn how reindeer and other mammoth-steppe megafauna have adapted their foraging behavior to changes in vegetation cover. In turn, this knowledge could help us understand and

predict how arctic herbivores might react to environmental changes due to climate change in the near future.

Acknowledgements

This work was funded by Norwegian Research Council award number 325589 to M.D.M. We thank Adrian Forsythe, Jørgen Rosvold and Laurène Lecaudey for assistance with sample collection. Furthermore, we thank the staff of the Musée National de Préhistoire, and especially Stéphane Madeleine and Jean-Jacques Cleyet-Merle, for assisting with sample acquisition and giving us the opportunity to conduct research on their material. Finally, we thank Reidar Andersen and Hans Stenøien for providing inspiration and logistical support to pursue this work on the French reindeer.

References

Alneberg, Johannes, Brynjar Smári Bjarnason, Ino de Bruijn, Melanie Schirmer, Joshua Quick, Umer Z. Ijaz, Leo Lahti, Nicholas J. Loman, Anders F. Andersson, and Christopher Quince. 2014. “Binning Metagenomic Contigs by Coverage and Composition.” *Nature Methods* 11 (11): 1144–46.

Amin, Nida, Sarah Schwarzkopf, Asako Kinoshita, Johanna Tröscher-Mußotter, Sven Dänicke, Amélia Camarinha-Silva, Korinna Huber, Jana Frahm, and Jana Seifert. 2021. “Evolution of Rumen and Oral Microbiota in Calves Is Influenced by Age and Time of Weaning.” *Animal Microbiome* 3 (1): 31.

Bengtsson-Palme, Johan, Erik Kristiansson, and D. G. Joakim Larsson. 2018. “Environmental Factors Influencing the Development and Spread of Antibiotic Resistance.” *FEMS Microbiology Reviews* 42 (1). https://doi.org/10.1093/femsre/fux053.

Blanchet, F., R. Kindt, P. Legendre, P. Minchin, and R. O’Hara. 2022. “Vegan: Community Ecology Package (R Package Version 2.6-2). 2022.” *Google Scholar There Is No*.

Borry, Maxime, Alexander Hübner, Adam B. Rohrlach, and Christina Warinner. 2021. “PyDamage: Automated Ancient Damage Identification and Estimation for Contigs in Ancient DNA de Novo Assembly.” *PeerJ* 9 (July): e11845.

Boyle, Katherine V. 1993. “Upper Palaeolithic Procurement and Processing Strategies in Southwest France.” *Archeological Papers of the American Anthropological Association* 4 (1): 151–62.

Brealey, Jaelle C., Henrique G. Leitão, Thijs Hofstede, Daniela C. Kalthoff, and Katerina Guschanski. 2021. “The Oral Microbiota of Wild Bears in Sweden Reflects the History of Antibiotic Use by Humans.” *Current Biology: CB* 31 (20): 4650–58.e6.

Brealey, Jaelle C., Henrique G. Leitão, Tom van der Valk, Wenbo Xu, Katia Bougiouri, Love Dalén, and Katerina Guschanski. 2020. “Dental Calculus as a Tool to Study the Evolution of the Mammalian Oral Microbiome.” *Molecular Biology and Evolution* 37 (10): 3003–22.

Briggs, Adrian W., Udo Stenzel, Philip L. F. Johnson, Richard E. Green, Janet Kelso, Kay Prüfer, Matthias Meyer, et al. 2007. “Patterns of Damage in Genomic DNA Sequences from a Neandertal.” *Proceedings of the National Academy of Sciences of the United States of America* 104 (37): 14616–21.

Britton, Kate, Elodie-Laure Jimenez, Mael Le Corre, Sylvain Renou, William Rendu, Michael P. Richards, Jean-Jacques Hublin, and Marie Soressi. 2023. “Multi-Isotope Analysis of Bone Collagen of Late Pleistocene Ungulates Reveals Niche Partitioning and Behavioural Plasticity of Reindeer during MIS 3.” *Scientific Reports* 13 (1): 15722.

Burch, Ernest S. 1972. “The Caribou/Wild Reindeer as a Human Resource.” *American Antiquity* 37 (3): 339–68.

Cao, Yifan, Marc Foggin, and Xinquan Zhao. 2022. “Tibetan Antelope Migration during Mass Calving as Parasite Avoidance Strategy.” *Innovation (Cambridge (Mass.))* 3 (6): 100326.

Chaumeil, Pierre-Alain, Aaron J. Mussig, Philip Hugenholtz, and Donovan H. Parks. 2019. “GTDB-Tk: A Toolkit to Classify Genomes with the Genome Taxonomy Database.” *Bioinformatics* 36 (6): 1925–27.

———. 2022. “GTDB-Tk v2: Memory Friendly Classification with the Genome Taxonomy Database.” *Bioinformatics* 38 (23): 5315–16.

Dabney, Jesse, Michael Knapp, Isabelle Glocke, Marie-Theres Gansauge, Antje Weihmann, Birgit Nickel, Cristina Valdiosera, et al. 2013. “Complete Mitochondrial Genome Sequence of a Middle Pleistocene Cave Bear

Reconstructed from Ultrashort DNA Fragments." *Proceedings of the National Academy of Sciences of the United States of America* 110 (39): 15758–63.
Davis, Nicole M., Diana M. Proctor, Susan P. Holmes, David A. Relman, and Benjamin J. Callahan. 2018. "Simple Statistical Identification and Removal of Contaminant Sequences in Marker-Gene and Metagenomics Data." *Microbiome* 6 (1): 226.
Duitama González, Camila, Riccardo Vicedomini, Téo Lemane, Nicolas Rascovan, Hugues Richard, and Rayan Chikhi. 2023. "decOM: Similarity-Based Microbial Source Tracking of Ancient Oral Samples Using K-Mer-Based Methods." *Microbiome* 11 (1): 243.
Eisenhofer, Raphael, Jeremiah J. Minich, Clarisse Marotz, Alan Cooper, Rob Knight, and Laura S. Weyrich. 2019. "Contamination in Low Microbial Biomass Microbiome Studies: Issues and Recommendations." *Trends in Microbiology* 27 (2): 105–17.
Eren, A. Murat, Evan Kiefl, Alon Shaiber, Iva Veseli, Samuel E. Miller, Matthew S. Schechter, Isaac Fink, et al. 2021. "Community-Led, Integrated, Reproducible Multi-Omics with Anvi'o." *Nature Microbiology* 6 (1): 3–6.
Ewels, Philip A., Alexander Peltzer, Sven Fillinger, Harshil Patel, Johannes Alneberg, Andreas Wilm, Maxime Ulysse Garcia, Paolo Di Tommaso, and Sven Nahnsen. 2020. "The Nf-Core Framework for Community-Curated Bioinformatics Pipelines." *Nature Biotechnology* 38 (3): 276–78.
Feuerborn, Tatiana R., Eleftheria Palkopoulou, Tom van der Valk, Johanna von Seth, Arielle R. Munters, Patrícia Pečnerová, Marianne Dehasque, et al. 2020. "Competitive Mapping Allows for the Identification and Exclusion of Human DNA Contamination in Ancient Faunal Genomic Datasets." *BMC Genomics* 21 (1): 844.
Flagstad, Øystein, and Knut H. Røed. 2003. "Refugial Origins of Reindeer (Rangifer Tarandus L.) Inferred from Mitochondrial DNA Sequences." *Evolution; International Journal of Organic Evolution* 57 (3): 658–70.
Frey, J. C., A. N. Pell, R. Berthiaume, H. Lapierre, S. Lee, J. K. Ha, J. E. Mendell, and E. R. Angert. 2010. "Comparative Studies of Microbial Populations in the Rumen, Duodenum, Ileum and Faeces of Lactating Dairy Cows." *Journal of Applied Microbiology* 108 (6): 1982–93.
Frioux, Clémence, Dipali Singh, Tamas Korcsmaros, and Falk Hildebrand. 2020. "From Bag-of-Genes to Bag-of-Genomes: Metabolic Modelling of Communities in the Era of Metagenome-Assembled Genomes." *Computational and Structural Biotechnology Journal* 18 (June): 1722–34.
Gaudzinski, S., and W. Roebroeks. 2000. "Adults Only. Reindeer Hunting at the Middle Palaeolithic Site Salzgitter Lebenstedt, Northern Germany." *Journal of Human Evolution* 38 (4): 497–521.
Gharechahi, Javad, Mohammad Farhad Vahidi, Mohammad Bahram, Jian-Lin Han, Xue-Zhi Ding, and Ghasem Hosseini Salekdeh. 2021. "Metagenomic Analysis Reveals a Dynamic Microbiome with Diversified Adaptive Functions to Utilize High Lignocellulosic Forages in the Cattle Rumen." *The ISME Journal* 15 (4): 1108–20.
Glendinning, Laura, Buğra Genç, R. John Wallace, and Mick Watson. 2021. "Metagenomic Analysis of the Cow, Sheep, Reindeer and Red Deer Rumen." *Scientific Reports* 11 (1): 1990.
Granehäll, Lena, Kun D. Huang, Adrian Tett, Paolo Manghi, Alice Paladin, Niall O'Sullivan, Omar Rota-Stabelli, Nicola Segata, Albert Zink, and Frank Maixner. 2021. "Metagenomic Analysis of Ancient Dental Calculus Reveals Unexplored Diversity of Oral Archaeal Methanobrevibacter." *Microbiome* 9 (1): 197.
Gylswyk, N. O. van. 1995. "Succiniclasticum Ruminis Gen. Nov., Sp. Nov., a Ruminal Bacterium Converting Succinate to Propionate as the Sole Energy-Yielding Mechanism." *International Journal of Systematic Bacteriology* 45 (2): 297–300.
Hyatt, Doug, Gwo-Liang Chen, Philip F. Locascio, Miriam L. Land, Frank W. Larimer, and Loren J. Hauser. 2010. "Prodigal: Prokaryotic Gene Recognition and Translation Initiation Site Identification." *BMC Bioinformatics* 11 (March): 119.
Jin, Ye, and Hak-Kong Yip. 2002. "Supragingival Calculus: Formation and Control." *Critical Reviews in Oral Biology and Medicine: An Official Publication of the American Association of Oral Biologists* 13 (5): 426–41.
Jónsson, Hákon, Aurélien Ginolhac, Mikkel Schubert, Philip L. F. Johnson, and Ludovic Orlando. 2013. "mapDamage2.0: Fast Approximate Bayesian Estimates of Ancient DNA Damage Parameters." *Bioinformatics* 29 (13): 1682–84.
Kamenova, Stefaniya, Eric J. de Muinck, Vebjørn Veiberg, Tove Aagnes Utsi, Sam M. J. G. Steyaert, Steve D. Albon, Leif Egil Loe, and Pål Trosvik. 2023. "Gut Microbiome Biogeography in Reindeer Supersedes Millennia of Ecological and Evolutionary Separation." *FEMS Microbiology Ecology* 99 (12). https://doi.org/10.1093/femsec/fiad157.
Kanehisa, M., and S. Goto. 2000. "KEGG: Kyoto Encyclopedia of Genes and Genomes." *Nucleic Acids Research* 28 (1): 27–30.
Kang, Dongwan, Jeff Froula, Rob Egan, and Zhong Wang. 2014. "MetaBAT: Metagenome Binning Based on Abundance and Tetranucleotide Frequence," March. https://escholarship.org/uc/item/1wz6h4fc.
Kapp, Joshua D., Richard E. Green, and Beth Shapiro. 2021. "A Fast and Efficient Single-Stranded Genomic Library Preparation Method Optimized for Ancient DNA." *The Journal of Heredity* 112 (3): 241–49.
Karkman, Antti, Katariina Pärnänen, and D. G. Joakim Larsson. 2019. "Fecal Pollution Can Explain Antibiotic Resistance Gene Abundances in Anthropogenically Impacted Environments." *Nature Communications* 10 (1): 80.
Key, Felix M., Cosimo Posth, Johannes Krause, Alexander Herbig, and Kirsten I. Bos. 2017. "Mining Metagenomic

Data Sets for Ancient DNA: Recommended Protocols for Authentication." *Trends in Genetics: TIG* 33 (8): 508–20.
Kircher, Martin, Susanna Sawyer, and Matthias Meyer. 2012. "Double Indexing Overcomes Inaccuracies in Multiplex Sequencing on the Illumina Platform." *Nucleic Acids Research* 40 (1): e3.
Kittelmann, Sandra, Michelle R. Kirk, Arjan Jonker, Alan McCulloch, and Peter H. Janssen. 2015. "Buccal Swabbing as a Noninvasive Method to Determine Bacterial, Archaeal, and Eukaryotic Microbial Community Structures in the Rumen." *Applied and Environmental Microbiology* 81 (21): 7470–83.
Klapper, Martin, Alexander Hübner, Anan Ibrahim, Ina Wasmuth, Maxime Borry, Veit G. Haensch, Shuaibing Zhang, et al. 2023. "Natural Products from Reconstructed Bacterial Genomes of the Middle and Upper Paleolithic." *Science* 380 (6645): 619–24.
Kolde, R. 2019. "Pheatmap: Pretty Heatmaps. Url: https://CRAN." *R-Project Org/package= Pheatmap*.
Kolenbrander Paul E., Andersen Roxanna N., Blehert David S., Egland Paul G., Foster Jamie S., and Palmer Robert J. 2002. "Communication among Oral Bacteria." *Microbiology and Molecular Biology Reviews: MMBR* 66 (3): 486–505.
Krakau, Sabrina, Daniel Straub, Hadrien Gourlé, Gisela Gabernet, and Sven Nahnsen. 2022. "Nf-Core/mag: A Best-Practice Pipeline for Metagenome Hybrid Assembly and Binning." *NAR Genomics and Bioinformatics* 4 (1): lqac007.
Kuhnert, Peter, Edzard Scholten, Stefan Haefner, Désirée Mayor, and Joachim Frey. 2010. "Basfia Succiniciproducens Gen. Nov., Sp. Nov., a New Member of the Family Pasteurellaceae Isolated from Bovine Rumen." *International Journal of Systematic and Evolutionary Microbiology* 60 (Pt 1): 44–50.
Kuntz, Delphine, and Sandrine Costamagno. 2011. "Relationships between Reindeer and Man in Southwestern France during the Magdalenian." *Quaternary International: The Journal of the International Union for Quaternary Research* 238 (1-2): 12–24.
Lee, Yun Kyung, and Sarkis K. Mazmanian. 2010. "Has the Microbiota Played a Critical Role in the Evolution of the Adaptive Immune System?" *Science* 330 (6012): 1768–73.
Legendre, P., and L. Legendre. 1998. "1998. Numerical Ecology." *Second English Edition. Elsevier, Amsterdam*.
Liang, Renxing, Maggie C. Y. Lau, Evan T. Saitta, Zachary K. Garvin, and Tullis C. Onstott. 2020. "Genome-Centric Resolution of Novel Microbial Lineages in an Excavated Centrosaurus Dinosaur Fossil Bone from the Late Cretaceous of North America." *Environmental Microbiome* 15 (1): 8.
Li, Dinghua, Chi-Man Liu, Ruibang Luo, Kunihiko Sadakane, and Tak-Wah Lam. 2015. "MEGAHIT: An Ultra-Fast Single-Node Solution for Large and Complex Metagenomics Assembly via Succinct de Bruijn Graph." *Bioinformatics* 31 (10): 1674–76.
Li, Heng. 2013. "Aligning Sequence Reads, Clone Sequences and Assembly Contigs with BWA-MEM." *arXiv [q-bio.GN]*. arXiv. http://arxiv.org/abs/1303.3997.
Lin, Zeshan, Lei Chen, Xianqing Chen, Yingbin Zhong, Yue Yang, Wenhao Xia, Chang Liu, et al. 2019. "Biological Adaptations in the Arctic Cervid, the Reindeer (Rangifer Tarandus)." *Science* 364 (6446). https://doi.org/10.1126/science.aav6312.
Llamas, Bastien, Guido Valverde, Lars Fehren-Schmitz, Laura S. Weyrich, Alan Cooper, and Wolfgang Haak. 2017. "From the Field to the Laboratory: Controlling DNA Contamination in Human Ancient DNA Research in the High-Throughput Sequencing Era." *STAR: Science & Technology of Archaeological Research* 3 (1): 1–14.
Lorenzen, Eline D., David Nogués-Bravo, Ludovic Orlando, Jaco Weinstock, Jonas Binladen, Katharine A. Marske, Andrew Ugan, et al. 2011. "Species-Specific Responses of Late Quaternary Megafauna to Climate and Humans." *Nature* 479 (7373): 359–64.
Mallick, Himel, Ali Rahnavard, Lauren J. McIver, Siyuan Ma, Yancong Zhang, Long H. Nguyen, Timothy L. Tickle, et al. 2021. "Multivariable Association Discovery in Population-Scale Meta-Omics Studies." *PLoS Computational Biology* 17 (11): e1009442.
Mann, Allison E., James A. Fellows Yates, Zandra Fagernäs, Rita M. Austin, Elizabeth A. Nelson, and Courtney A. Hofman. 2023. "Do I Have Something in My Teeth? The Trouble with Genetic Analyses of Diet from Archaeological Dental Calculus." *Quaternary International: The Journal of the International Union for Quaternary Research* 653-654 (April): 33–46.
Mann, Allison E., Susanna Sabin, Kirsten Ziesemer, Åshild J. Vågene, Hannes Schroeder, Andrew T. Ozga, Krithivasan Sankaranarayanan, et al. 2018. "Differential Preservation of Endogenous Human and Microbial DNA in Dental Calculus and Dentin." *Scientific Reports* 8 (1): 9822.
Maury, J., and J-A Le Bel. 1925. *Laugerie Basse : The Excavations of M.J.-A. Le Bel*. Translated by Arthur Edmunds. Le Mans: Monnoyer.
McFall-Ngai, Margaret J. 2002. "Unseen Forces: The Influence of Bacteria on Animal Development." *Developmental Biology* 242 (1): 1–14.
McMurdie, Paul J., and Susan Holmes. 2013. "Phyloseq: An R Package for Reproducible Interactive Analysis and Graphics of Microbiome Census Data." *PloS One* 8 (4): e61217.
Michelland, R. J., V. Monteils, A. Zened, S. Combes, L. Cauquil, T. Gidenne, J. Hamelin, and L. Fortun-Lamothe. 2009. "Spatial and Temporal Variations of the Bacterial Community in the Bovine Digestive Tract." *Journal of Applied Microbiology* 107 (5): 1642–50.

Mistry, Jaina, Sara Chuguransky, Lowri Williams, Matloob Qureshi, Gustavo A. Salazar, Erik L. L. Sonnhammer, Silvio C. E. Tosatto, et al. 2021. “Pfam: The Protein Families Database in 2021.” *Nucleic Acids Research* 49 (D1): D412–19.
Modi, Alessandra, Lisa Pisaneschi, Valentina Zaro, Stefania Vai, Chiara Vergata, Enrico Casalone, David Caramelli, Jacopo Moggi-Cecchi, Marta Mariotti Lippi, and Martina Lari. 2020. “Combined Methodologies for Gaining Much Information from Ancient Dental Calculus: Testing Experimental Strategies for Simultaneously Analysing DNA and Food Residues.” *Archaeological and Anthropological Sciences* 12 (1). https://doi.org/10.1007/s12520-019-00983-5.
Molin, G., and A. Ternstrom. 1986. “Phenotypically Based Taxonomy of Psychrotrophic Pseudomonas Isolated from Spoiled Meat, Water, and Soil.” *International Journal of Systematic Bacteriology* 36 (2): 257–74.
Molin, G., A. Ternstrom, and J. Ursing. 1986. “Notes: Pseudomonas Lundensis, a New Bacterial Species Isolated from Meat.” *International Journal of Systematic Bacteriology* 36 (2): 339–42.
Moraitou, Markella, Adrian Forsythe, James A. Fellows Yates, Jaelle C. Brealey, Christina Warinner, and Katerina Guschanski. 2022. “Ecology, Not Host Phylogeny, Shapes the Oral Microbiome in Closely Related Species.” *Molecular Biology and Evolution* 39 (12). https://doi.org/10.1093/molbev/msac263.
Müller-Wille, L., D. Heinrich, V-P Lehtola, P. Aikio, Y. Konstantinov, and V. Vladimirova. 2006. “Dynamics in Human-Reindeer Relations: Reflections on Prehistoric, Historic and Contemporary Practices in Northernmost Europe.” In *Reindeer Management in Northernmost Europe: Linking Practical and Scientific Knowledge in Social-Ecological Systems*, edited by Bruce C. Forbes, Manfred Bölter, Ludger Müller-Wille, Janne Hukkinen, Felix Müller, Nicolas Gunslay, and Yulian Konstantinov, 27–45. Berlin, Heidelberg: Springer Berlin Heidelberg.
Nichols, Robert G., Jeffrey M. Peters, and Andrew D. Patterson. 2019. “Interplay Between the Host, the Human Microbiome, and Drug Metabolism.” *Human Genomics* 13 (1): 27.
Nieuwdorp, Max, Pim W. Gilijamse, Nikhil Pai, and Lee M. Kaplan. 2014. “Role of the Microbiome in Energy Regulation and Metabolism.” *Gastroenterology* 146 (6): 1525–33.
Nikitakis, N. G., W. Papaioannou, L. I. Sakkas, and E. Kousvelari. 2017. “The Autoimmunity-Oral Microbiome Connection.” *Oral Diseases* 23 (7): 828–39.
Niven, Laura, Teresa E. Steele, William Rendu, Jean-Baptiste Mallye, Shannon P. McPherron, Marie Soressi, Jacques Jaubert, and Jean-Jacques Hublin. 2012. “Neandertal Mobility and Large-Game Hunting: The Exploitation of Reindeer during the Quina Mousterian at Chez-Pinaud Jonzac (Charente-Maritime, France).” *Journal of Human Evolution* 63 (4): 624–35.
Oliveira, Marcelo Nagem Valério de, Kelsea A. Jewell, Fernanda S. Freitas, Laércio A. Benjamin, Marcos R. Tótola, Arnaldo C. Borges, Célia A. Moraes, and Garret Suen. 2013. “Characterizing the Microbiota across the Gastrointestinal Tract of a Brazilian Nelore Steer.” *Veterinary Microbiology* 164 (3-4): 307–14.
Olm, Matthew R., Christopher T. Brown, Brandon Brooks, and Jillian F. Banfield. 2017. “dRep: A Tool for Fast and Accurate Genomic Comparisons That Enables Improved Genome Recovery from Metagenomes through de-Replication.” *The ISME Journal* 11 (12): 2864–68.
Ondov, Brian D., Todd J. Treangen, Páll Melsted, Adam B. Mallonee, Nicholas H. Bergman, Sergey Koren, and Adam M. Phillippy. 2016. “Mash: Fast Genome and Metagenome Distance Estimation Using MinHash.” *Genome Biology* 17 (1): 132.
Østbye, Kjartan, Robert Wilson, and Knut Rudi. 2016. “Rumen Microbiota for Wild Boreal Cervids Living in the Same Habitat.” *FEMS Microbiology Letters* 363 (20). https://doi.org/10.1093/femsle/fnw233.
Ottoni, Claudio, Meriam Guellil, Andrew T. Ozga, Anne C. Stone, Oliver Kersten, Barbara Bramanti, Stéphanie Porcier, and Wim Van Neer. 2019. “Metagenomic Analysis of Dental Calculus in Ancient Egyptian Baboons.” *Scientific Reports* 9 (1): 1–10.
Ozga, Andrew T., and Claudio Ottoni. 2023. “Dental Calculus as a Proxy for Animal Microbiomes.” *Quaternary International: The Journal of the International Union for Quaternary Research* 653-654 (April): 47–52.
Paradis, Emmanuel, and Klaus Schliep. 2019. “Ape 5.0: An Environment for Modern Phylogenetics and Evolutionary Analyses in R.” *Bioinformatics* 35 (3): 526–28.
Parks, Donovan H., Michael Imelfort, Connor T. Skennerton, Philip Hugenholtz, and Gene W. Tyson. 2015. “CheckM: Assessing the Quality of Microbial Genomes Recovered from Isolates, Single Cells, and Metagenomes.” *Genome Research* 25 (7): 1043–55.
Peng, Xuefeng, St Elmo Wilken, Thomas S. Lankiewicz, Sean P. Gilmore, Jennifer L. Brown, John K. Henske, Candice L. Swift, et al. 2021. “Genomic and Functional Analyses of Fungal and Bacterial Consortia That Enable Lignocellulose Breakdown in Goat Gut Microbiomes.” *Nature Microbiology* 6 (4): 499–511.
Pope, Phillip B., Alasdair K. Mackenzie, Ivan Gregor, Wendy Smith, Monica A. Sundset, Alice C. McHardy, Mark Morrison, and Vincent G. H. Eijsink. 2012. “Metagenomics of the Svalbard Reindeer Rumen Microbiome Reveals Abundance of Polysaccharide Utilization Loci.” *PloS One* 7 (6): e38571.
Prüfer, Kay, Udo Stenzel, Michael Hofreiter, Svante Pääbo, Janet Kelso, and Richard E. Green. 2010. “Computational Challenges in the Analysis of Ancient DNA.” *Genome Biology* 11 (5): R47.
Ramberg, Per, Satoshi Sekino, Naciye Guzin Uzel, Sigmund Socransky, and Jan Lindhe. 2003. “Bacterial Colonization during de Novo Plaque Formation.” *Journal of Clinical Periodontology* 30 (11): 990–95.
R Core Team. 2021. “R: A Language and Environment for Statistical Computing.” Vienna, Austria: R Foundation for

Statistical Computing. https://www.R-project.org/.
Richter, Michael, and Ramon Rosselló-Móra. 2009. “Shifting the Genomic Gold Standard for the Prokaryotic Species Definition.” *Proceedings of the National Academy of Sciences of the United States of America* 106 (45): 19126–31.
Rinke, Christian, Patrick Schwientek, Alexander Sczyrba, Natalia N. Ivanova, Iain J. Anderson, Jan-Fang Cheng, Aaron Darling, et al. 2013. “Insights into the Phylogeny and Coding Potential of Microbial Dark Matter.” *Nature* 499 (7459): 431–37.
Rosenberg, Eugene, and Ilana Zilber-Rosenberg. 2018. “The Hologenome Concept of Evolution after 10 Years.” *Microbiome* 6 (1): 78.
Saitta, Evan T., Renxing Liang, Maggie C. Y. Lau, Caleb M. Brown, Nicholas R. Longrich, Thomas G. Kaye, Ben J. Novak, et al. 2019. “Cretaceous Dinosaur Bone Contains Recent Organic Material and Provides an Environment Conducive to Microbial Communities.” *eLife* 8. https://doi.org/10.7554/elife.46205.
Salgado-Flores, Alejandro, Live H. Hagen, Suzanne L. Ishaq, Mirzaman Zamanzadeh, André-Denis G. Wright, Phillip B. Pope, and Monica A. Sundset. 2016. “Rumen and Cecum Microbiomes in Reindeer (Rangifer Tarandus Tarandus) Are Changed in Response to a Lichen Diet and May Affect Enteric Methane Emissions.” *PloS One* 11 (5): e0155213.
Salter, Susannah J., Michael J. Cox, Elena M. Turek, Szymon T. Calus, William O. Cookson, Miriam F. Moffatt, Paul Turner, Julian Parkhill, Nicholas J. Loman, and Alan W. Walker. 2014. “Reagent and Laboratory Contamination Can Critically Impact Sequence-Based Microbiome Analyses.” *BMC Biology* 12 (November): 87.
Schubert, Mikkel, Luca Ermini, Clio Der Sarkissian, Hákon Jónsson, Aurélien Ginolhac, Robert Schaefer, Michael D. Martin, et al. 2014. “Characterization of Ancient and Modern Genomes by SNP Detection and Phylogenomic and Metagenomic Analysis Using PALEOMIX.” *Nature Protocols* 9 (5): 1056–82.
Scott, Carly B., Anny Cárdenas, Matthew Mah, Vagheesh M. Narasimhan, Nadin Rohland, Lauren T. Toth, Christian R. Voolstra, David Reich, and Mikhail V. Matz. 2022. “Millennia-Old Coral Holobiont DNA Provides Insight into Future Adaptive Trajectories.” *Molecular Ecology* 31 (19): 4979–90.
Sommer, Robert S., Johannes Kalbe, Jonas Ekström, Norbert Benecke, and Ronnie Liljegren. 2014. “Range Dynamics of the Reindeer in Europe during the Last 25,000 Years.” *Journal of Biogeography* 41 (2): 298–306.
Stewart, Robert D., Marc D. Auffret, Amanda Warr, Andrew H. Wiser, Maximilian O. Press, Kyle W. Langford, Ivan Liachko, et al. 2018. “Assembly of 913 Microbial Genomes from Metagenomic Sequencing of the Cow Rumen.” *Nature Communications* 9 (1): 870.
Stien, A., R. J. Irvine, E. Ropstad, O. Halvorsen, R. Langvatn, and S. D. Albon. 2002. “The Impact of Gastrointestinal Nematodes on Wild Reindeer: Experimental and Cross‐sectional Studies.” *The Journal of Animal Ecology* 71 (6): 937–45.
Sundset, Monica A., Joan E. Edwards, Yan Fen Cheng, Roberto S. Senosiain, Maria N. Fraile, Korinne S. Northwood, Kirsti E. Praesteng, Trine Glad, Svein D. Mathiesen, and André-Denis G. Wright. 2009. “Molecular Diversity of the Rumen Microbiome of Norwegian Reindeer on Natural Summer Pasture.” *Microbial Ecology* 57 (2): 335–48.
Tapio, Ilma, Kevin J. Shingfield, Nest McKain, Aurélie Bonin, Daniel Fischer, Ali R. Bayat, Johanna Vilkki, Pierre Taberlet, Timothy J. Snelling, and R. John Wallace. 2016. “Oral Samples as Non-Invasive Proxies for Assessing the Composition of the Rumen Microbial Community.” *PloS One* 11 (3): e0151220.
Taylor, Rebecca S., Rebekah L. Horn, Xi Zhang, G. Brian Golding, Micheline Manseau, and Paul J. Wilson. 2019. “The Caribou (Rangifer Tarandus) Genome.” *Genes* 10 (7): 540.
Tian, Zhi, Shan Lu, Dong Jin, Jing Yang, Ji Pu, Xin-He Lai, Xiang-Ning Bai, et al. 2019. “Streptococcus Chenjunshii Sp. Nov. Isolated from Feces of Tibetan Antelopes.” *International Journal of Systematic and Evolutionary Microbiology* 69 (4): 1237–43.
Uritskiy, Gherman V., Jocelyne DiRuggiero, and James Taylor. 2018. “MetaWRAP-a Flexible Pipeline for Genome-Resolved Metagenomic Data Analysis.” *Microbiome* 6 (1): 158.
Utter, Daniel R., Jessica L. Mark Welch, and Gary G. Borisy. 2016. “Individuality, Stability, and Variability of the Plaque Microbiome.” *Frontiers in Microbiology* 7 (April): 564.
Vaidya, Jueeli D., Bastian V. H. Hornung, Hauke Smidt, Joan E. Edwards, and Caroline M. Plugge. 2019. “Propionibacterium Ruminifibrarum Sp. Nov., Isolated from Cow Rumen Fibrous Content.” *International Journal of Systematic and Evolutionary Microbiology* 69 (8): 2584–90.
Veiberg, Vebjørn, Erlend B. Nilsen, Christer M. Rolandsen, Morten Heim, Roy Andersen, Frode Holmstrøm, Erling L. Meisingset, and Erling J. Solberg. 2020. “The Accuracy and Precision of Age Determination by Dental Cementum Annuli in Four Northern Cervids.” *European Journal of Wildlife Research* 66 (6): 91.
Velsko, Irina M., Laurent A. F. Frantz, Alexander Herbig, Greger Larson, and Christina Warinner. 2018. “Selection of Appropriate Metagenome Taxonomic Classifiers for Ancient Microbiome Research.” *mSystems* 3 (4): 1–23.
Warinner, Christina, Alexander Herbig, Allison Mann, James A. Fellows Yates, Clemens L. Weiß, Hernán A. Burbano, Ludovic Orlando, and Johannes Krause. 2017. “A Robust Framework for Microbial Archaeology.” *Annual Review of Genomics and Human Genetics* 18 (1): 321–56.
Warinner, Christina, João F. Matias Rodrigues, Rounak Vyas, Christian Trachsel, Natallia Shved, Jonas Grossmann, Anita Radini, et al. 2014. “Pathogens and Host Immunity in the Ancient Human Oral Cavity.” *Nature Genetics* 46

(4): 336–44.
Warinner, Christina, Camilla Speller, and Matthew J. Collins. 2015. “A New Era in Palaeomicrobiology: Prospects for Ancient Dental Calculus as a Long-Term Record of the Human Oral Microbiome.” *Philosophical Transactions of the Royal Society of London. Series B, Biological Sciences* 370 (1660): 20130376.
Wei, Ziqian, Zengrang Xu, Tian Qiao, Shouxing Wang, Natarajan Ishwaran, and Mingxin Yang. 2023. “Habitats Change of Tibetan Antelope and Its Influencing Factors on the North Tibetan Plateau from 2020 to 2050.” *Global Ecology and Conservation* 43 (June): e02462.
Wickham, Hadley, Winston Chang, and Maintainer Hadley Wickham. 2016. “Package ‘ggplot2.’” *Create Elegant Data Visualisations Using the Grammar of Graphics. Version* 2 (1): 1–189.
Wu, Yu-Wei, Blake A. Simmons, and Steven W. Singer. 2016. “MaxBin 2.0: An Automated Binning Algorithm to Recover Genomes from Multiple Metagenomic Datasets.” *Bioinformatics* 32 (4): 605–7.
Yang, Dongya Y., and Kathy Watt. 2005. “Contamination Controls When Preparing Archaeological Remains for Ancient DNA Analysis.” *Journal of Archaeological Science* 32 (3): 331–36.
Yannic, Glenn, Joaquín Ortego, Loïc Pellissier, Nicolas Lecomte, Louis Bernatchez, and Steeve D. Côté. 2018. “Linking Genetic and Ecological Differentiation in an Ungulate with a Circumpolar Distribution.” *Ecography* 41 (6): 922–37.
Yates, James A. Fellows, Irina M. Velsko, Franziska Aron, Cosimo Posth, Courtney A. Hofman, Rita M. Austin, Cody E. Parker, et al. 2021. “The Evolution and Changing Ecology of the African Hominid Oral Microbiome.” *Proceedings of the National Academy of Sciences* 118 (20): e2021655118.
Zielińska, Sylwia, Dorota Kidawa, Lech Stempniewicz, Marcin Łoś, and Joanna M. Łoś. 2016. “New Insights into the Microbiota of the Svalbard Reindeer Rangifer Tarandus Platyrhynchus.” *Frontiers in Microbiology* 7 (February): 170.
Ziesemer, Kirsten A., Allison E. Mann, Krithivasan Sankaranarayanan, Hannes Schroeder, Andrew T. Ozga, Bernd W. Brandt, Egija Zaura, et al. 2015. “Intrinsic Challenges in Ancient Microbiome Reconstruction Using 16S rRNA Gene Amplification.” *Scientific Reports* 5 (November): 16498.

Supplementary Material / Appendix

Supplementary Table 1: Overview over all assembled metagenome-assembled genomes (MAGs). Abundance is filtered for detection (minimum 0.3) and summed up across all samples. If detection is below the threshold, abundance is set to 0 (= not present). Completion, redundancy (contamination), GC content, N_{50} and total length were calculated with checkM (Parks et al. 2015). Taxa which were identified as lab contaminants with decontam (Davis et al. 2018) are removed.

Co-Assembly batch	BIN	OTU	Sum abundance	Completion [%]	Contamination [%]	GC [%]	N50	Total length [bp]	domain	phylum	class	order	family	genus	species
MODERN	bin_32_mod	Actinomyces sp.	91.6	96.4	2.2	70.5	30226	3644339	Bacteria	Actinobacteriota	Actinomycetia	Actinomycetales	Actinomycetaceae	Actinomyces	
MODERN	bin_61_mod	Actinomyces sp.	186.7	81.4	6.6	67.2	9587	3175201	Bacteria	Actinobacteriota	Actinomycetia	Actinomycetales	Actinomycetaceae	Actinomyces	
MODERN	bin_46_mod	Actinomyces sp.	35.6	53.8	2.4	69	4500	1828876	Bacteria	Actinobacteriota	Actinomycetia	Actinomycetales	Actinomycetaceae	Actinomyces	
ANCIENT	bin_19_anc	Allosaccharopolyspora sp.	12.5	86.3	6.0	67.7	21599	4697505	Bacteria	Actinobacteriota	Actinomycetia	Mycobacteriales	Pseudonocardiaceae	Allosaccharopolyspora	
ANCIENT	bin_23_anc	Allosaccharopolyspora sp	14.5	80.9	3.9	66.7	18237	4092176	Bacteria	Actinobacteriota	Actinomycetia	Mycobacteriales	Pseudonocardiaceae	Allosaccharopolyspora	
ANCIENT	bin_3_anc	Allosaccharopolyspora sp	48.6	60.8	8.6	69.3	3491	5315633	Bacteria	Actinobacteriota	Actinomycetia	Mycobacteriales	Pseudonocardiaceae	Allosaccharopolyspora	
ANCIENT	bin_35_anc	Allosaccharopolyspora sp	18.3	85.4	6.8	68.7	17034	4732674	Bacteria	Actinobacteriota	Actinomycetia	Mycobacteriales	Pseudonocardiaceae	Allosaccharopolyspora	

Co-Assembly batch	BIN	OTU	Sum abundance	Completion [%]	Contamination [%]	GC [%]	N50	Total length [bp]	domain	phylum	class	order	family	genus	species
ANCIENT	bin_48_anc	Allosaccharopolyspora sp	5.2	63.7	3.7	66.3	3925	4738523	Bacteria	Actinobacteriota	Actinomycetia	Mycobacteriales	Pseudonocardiaceae	Allosaccharopolyspora	
ANCIENT	bin_6_anc	Amycolatopsis_C sp009377395	9.7	51.2	0.0	70.2	4322	3353510	Bacteria	Actinobacteriota	Actinomycetia	Mycobacteriales	Pseudonocardiaceae	Amycolatopsis_C	Amycolatopsis_C sp009377395
ANCIENT	bin_F_dup	Asp313 sp.	146.2	57.0	2.9	61.1	3104	1588855	Bacteria	Actinobacteriota	Actinomycetia	Actinomycetales	Actinomycetaceae	Asp313	
MODERN	bin_F_dup	Asp313 sp.	146.2	95.5	3.1	61.3	12465	2503362	Bacteria	Actinobacteriota	Actinomycetia	Actinomycetales	Actinomycetaceae	Asp313	
MODERN	bin_45_mod	Bacteroides sp.	9.0	97.6	0.1	47.6	60945	2853739	Bacteria	Bacteroidota	Bacteroidia	Bacteroidales	Bacteroidaceae	Bacteroides	
ANCIENT	bin_A_dup	Basfia_A sp.	162.7	86.5	4.5	44.6	3432	2032619	Bacteria	Proteobacteria	Gammaproteobacteria	Enterobacterales	Pasteurellaceae	Basfia_A	
MODERN	bin_A_dup	Basfia_A sp.	162.7	99.2	3.0	44.4	40885	2463674	Bacteria	Proteobacteria	Gammaproteobacteria	Enterobacterales	Pasteurellaceae	Basfia_A	
MODERN	bin_49_mod	Bibersteinia sp.	8.6	87.5	2.4	41.4	9861	1781199	Bacteria	Proteobacteria	Gammaproteobacteria	Enterobacterales	Pasteurellaceae	Bibersteinia	
ANCIENT	bin_45_anc	Bilifractor sp.	134.6	96.5	4.2	46.3	9104	2771729	Bacteria	Firmicutes_A	Clostridia	Lachnospirales	Lachnospiraceae	Bilifractor	
MODERN	bin_11_mod	Brachymonas sp.	14.0	91.8	1.3	51.1	20494	1932991	Bacteria	Proteobacteria	Gammaproteobacteria	Burkholderiales	Burkholderiaceae	Brachymonas	
ANCIENT	bin_3	CAG-791 sp.	61.6	74.0	8.0	51.4	2206	2210786	Bacteria	Firmicutes	Clostridia	Lachnospi	Lachnospi	CAG-791	

Co-Assembly batch	BIN	OTU	Sum abundance	Completion [%]	Contamination [%]	GC [%]	N50	Total length [bp]	domain	phylum	class	order	family	genus	species
	1_anc									_A		rales	raceae		
MODERN	bin_16_mod	CAJPNX01 sp.	6.7	71.0	1.5	51.8	3916	1346648	Bacteria	Proteobacteria	Gammaproteobacteria	Burkholderiales	Neisseriaceae	CAJPNX01	
MODERN	bin_30_mod	Campylobacter_B sp.	1.2	88.0	2.6	37	3773	1857269	Bacteria	Campylobacterota	Campylobacteria	Campylobacterales	Campylobacteraceae	Campylobacter_B	
MODERN	bin_22_mod	Chryseobacterium piscium	1.6	51.3	2.0	38.4	1507	2718075	Bacteria	Bacteroidota	Bacteroidia	Flavobacteriales	Weeksellaceae	Chryseobacterium	Chryseobacterium piscium
MODERN	bin_29_mod	Cryptobacteroides sp.	10.8	93.6	0.6	53.6	29385	1969542	Bacteria	Bacteroidota	Bacteroidia	Bacteroidales	UBA932	Cryptobacteroides	
MODERN	bin_54_mod	Cryptobacteroides sp	1.9	54.2	2.8	55.5	1621	1646386	Bacteria	Bacteroidota	Bacteroidia	Bacteroidales	UBA932	Cryptobacteroides	
ANCIENT	bin_58_anc	CSP1-5 sp.	1.4	56.3	15.0	64.9	1926	1462166	Bacteria	Methylomirabilota	Methylomirabilia	Methylomirabilales	CSP1-5	CSP1-5	
MODERN	bin_12_mod	Desulfovibrio desulfuricans_D	17.6	97.0	0.6	63.8	36484	2681036	Bacteria	Desulfobacterota_I	Desulfovibrionia	Desulfovibrionales	Desulfovibrionaceae	Desulfovibrio	Desulfovibrio desulfuricans_D
ANCIENT	bin_52_anc	DP-1 sp.	4.6	66.5	3.0	55.4	2224	5408552	Bacteria	Desulfobacterota_B	Binatia	UBA9968	UBA9968	DP-1	
MODERN	bin_18_mod	Eubacterium_I sp.	14.2	96.3	2.6	47.9	20511	2242840	Bacteria	Firmicutes_A	Clostridia	Lachnospirales	Lachnospiraceae	Eubacterium_I	
ANCIENT	bin_22_anc	Eubacterium_I sp	13.5	69.3	4.8	48.5	2388	1857276	Bacteria	Firmicutes_A	Clostridia	Lachnospirales	Lachnospiraceae	Eubacterium_I	

Co-Assembly batch	BIN	OTU	Sum abundance	Completion [%]	Contamination [%]	GC [%]	N50	Total length [bp]	domain	phylum	class	order	family	genus	species
MODERN	bin_20_mod	Flavobacterium sp.	1.9	54.9	1.5	38.2	1635	1813077	Bacteria	Bacteroidota	Bacteroidia	Flavobacteriales	Flavobacteriaceae	Flavobacterium	
MODERN	bin_21_mod	Flavobacterium sp	5.1	97.0	0.5	34	14395	3772220	Bacteria	Bacteroidota	Bacteroidia	Flavobacteriales	Flavobacteriaceae	Flavobacterium	
ANCIENT	bin_61_anc	Flavobacterium sp	53.2	68.9	2.2	33.5	2960	2292418	Bacteria	Bacteroidota	Bacteroidia	Flavobacteriales	Flavobacteriaceae	Flavobacterium	
MODERN	bin_10_mod	Fusobacterium sp.	3.3	75.6	4.0	27.7	4517	1610384	Bacteria	Fusobacteriota	Fusobacteriia	Fusobacteriales	Fusobacteriaceae	Fusobacterium	
MODERN	bin_15_mod	Fusobacterium sp	8.3	96.1	4.4	27.9	14777	2110346	Bacteria	Fusobacteriota	Fusobacteriia	Fusobacteriales	Fusobacteriaceae	Fusobacterium	
MODERN	bin_50_mod	Fusobacterium_C necrophorum	4.1	98.3	1.7	35.1	15284	2011259	Bacteria	Fusobacteriota	Fusobacteriia	Fusobacteriales	Fusobacteriaceae	Fusobacterium_C	Fusobacterium_C necrophorum
ANCIENT	bin_29_anc	Haemophilus_B sp.	72.5	93.3	3.0	46.5	9924	2121583	Bacteria	Proteobacteria	Gammaproteobacteria	Enterobacterales	Pasteurellaceae	Haemophilus_B	
ANCIENT	bin_11_anc	Homoserinimonas sp.	6.5	85.6	4.2	65	9895	2715953	Bacteria	Actinobacteriota	Actinomycetia	Actinomycetales	Microbacteriaceae	Homoserinimonas	
ANCIENT	bin_47_anc	Hornefia sp.	10.9	52.9	6.0	57	1448	1778449	Bacteria	Firmicutes_A	Clostridia	Peptostreptococcales	Anaerovoracaceae	Hornefia	
ANCIENT	bin_46_anc	JACQPT01 sp.	11.0	97.5	3.3	50.2	70727	4230797	Bacteria	Bacteroidota	UBA10030	UBA10030	UBA10030	JACQPT01	
MODERN	bin_2	JAGOWQ01	16.0	98.9	1.1	26.1	31295	1626520	Bacteria	Fusobacte	Fusobacte	Fusobacte	Leptotrichi	JAGOWQ	

Co-Assembly batch	BIN	OTU	Sum abundance	Completion [%]	Contamination [%]	GC [%]	N50	Total length [bp]	domain	phylum	class	order	family	genus	species
	4_mod	sp.								riota	riia	riales	aceae	01	
MODERN	bin_7_mod	JAGOWQ01 sp	130.7	95.5	2.2	30.1	20386	2117629	Bacteria	Fusobacteriota	Fusobacteriia	Fusobacteriales	Leptotrichiaceae	JAGOWQ01	
ANCIENT	bin_57_anc	Lactobacillaceae	10.8	52.7	2.5	27.6	4214	582164	Bacteria	Firmicutes	Bacilli	Lactobacillales	Lactobacillaceae		
ANCIENT	bin_49_anc	Lactobacillus intestinalis	18.8	76.3	0.1	35.7	4625	1284317	Bacteria	Firmicutes	Bacilli	Lactobacillales	Lactobacillaceae	Lactobacillus	Lactobacillus intestinalis
ANCIENT	bin_21_anc	Lactobacillus johnsonii	1.9	52.7	12.2	38	1287	1914068	Bacteria	Firmicutes	Bacilli	Lactobacillales	Lactobacillaceae	Lactobacillus	Lactobacillus johnsonii
MODERN	bin_51_mod	Lautropia sp.	91.5	90.9	7.2	62.3	6775	3509295	Bacteria	Proteobacteria	Gammaproteobacteria	Burkholderiales	Burkholderiaceae	Lautropia	
ANCIENT	bin_34_anc	Ligilactobacillus murinus	8.0	79.8	1.3	40.8	4129	1250582	Bacteria	Firmicutes	Bacilli	Lactobacillales	Lactobacillaceae	Ligilactobacillus	Ligilactobacillus murinus
MODERN	bin_3_mod	Mannheimia sp.	7.0	84.0	5.9	39.4	7821	1829725	Bacteria	Proteobacteria	Gammaproteobacteria	Enterobacterales	Pasteurellaceae	Mannheimia	
MODERN	bin_57_mod	Mannheimia sp	509.9	92.8	9.9	37.5	17334	1850535	Bacteria	Proteobacteria	Gammaproteobacteria	Enterobacterales	Pasteurellaceae	Mannheimia	
MODERN	bin_9_mod	Mesocricetibacter sp.	34.2	98.7	0.8	47.8	37339	2757061	Bacteria	Proteobacteria	Gammaproteobacteria	Enterobacterales	Pasteurellaceae	Mesocricetibacter	
ANCIENT	bin_38_anc	Methanobrevibacter sp.	50.1	71.0	2.4	32.7	4540	1560997	Archaea	Methanobacteriota	Methanobacteria	Methanobacteriales	Methanobacteriacea	Methanobrevibacter	

Co-Assembly batch	BIN	OTU	Sum abundance	Completion [%]	Contamination [%]	GC [%]	N50	Total length [bp]	domain	phylum	class	order	family	genus	species
													e		
ANCIENT	bin_33_anc	Methanobrevibacter_A sp.	18.1	85.7	5.7	30.6	7432	1973885	Archaea	Methanobacteriota	Methanobacteria	Methanobacteriales	Methanobacteriaceae	Methanobrevibacter_A	
ANCIENT	bin_41_anc	Methanobrevibacter_A sp	7.8	78.3	3.2	28.1	3608	1516164	Archaea	Methanobacteriota	Methanobacteria	Methanobacteriales	Methanobacteriaceae	Methanobrevibacter_A	
MODERN	bin_6_mod	Methanomethylophilus sp.	2.1	59.8	8.3	58.8	1678	2017389	Archaea	Thermoplasmatota	Thermoplasmata	Methanomassiliiococcales	Methanomethylophilaceae	Methanomethylophilus	
ANCIENT	bin_28_anc	Methanosphaera sp.	95.1	88.6	5.0	32.5	11685	1792003	Archaea	Methanobacteriota	Methanobacteria	Methanobacteriales	Methanobacteriaceae	Methanosphaera	
ANCIENT	bin_4_anc	Methanosphaera sp	51.6	84.4	2.9	27.8	10793	2063892	Archaea	Methanobacteriota	Methanobacteria	Methanobacteriales	Methanobacteriaceae	Methanosphaera	
ANCIENT	bin_42_anc	Nanosyncoccus sp.	6.1	56.9	0.2	43.2	5751	533024	Bacteria	Patescibacteria	Sacchari monadia	Sacchari monadales	Nanosyncoccaceae	Nanosyncoccus	
MODERN	bin_4_mod	Neisseria sp.	22.7	96.5	11.5	53.9	7616	2331604	Bacteria	Proteobacteria	Gammaproteobacteria	Burkholderiales	Neisseriaceae	Neisseria	
ANCIENT	bin_27_anc	NS-7 sp.	3.2	86.3	4.6	58.6	9995	2678817	Bacteria	Nitrospirota	Nitrospiria	Nitrospirales	Nitrospiraceae	NS-7	
ANCIENT	bin_9_anc	Oceanobacillus sp.	1.5	57.8	2.1	36.6	1756	3333676	Bacteria	Firmicutes	Bacilli	Bacillales_D	Amphibacillaceae	Oceanobacillus	
ANCIENT	bin_64_anc	Paenisporosarcina sp.	2.3	73.6	6.6	37.3	3419	3063473	Bacteria	Firmicutes	Bacilli	Bacillales_A	Planococcaceae	Paenisporosarcina	

Co-Assembly batch	BIN	OTU	Sum abundance	Completion [%]	Contamination [%]	GC [%]	N50	Total length [bp]	domain	phylum	class	order	family	genus	species
ANCIENT	bin_50_anc	Pararheinheimera sp.	3.4	77.1	0.0	52.4	4858	3828432	Bacteria	Proteobacteria	Gammaproteobacteria	Enterobacterales	Alteromonadaceae	Pararheinheimera	
ANCIENT	bin_63_anc	Pararheinheimera tangshanensis	1.7	68.2	4.0	46.6	2091	2670909	Bacteria	Proteobacteria	Gammaproteobacteria	Enterobacterales	Alteromonadaceae	Pararheinheimera	Pararheinheimera tangshanensis
MODERN	bin_34_mod	Peptidiphaga sp.	136.1	95.4	0.0	65.7	64087	2306248	Bacteria	Actinobacteriota	Actinomycetia	Actinomycetales	Actinomycetaceae	Peptidiphaga	
ANCIENT	bin_10_anc	Pontibacter sp.	3.1	90.7	2.4	44	9918	3941209	Bacteria	Bacteroidota	Bacteroidia	Cytophagales	Hymenobacteraceae	Pontibacter	
MODERN	bin_26_mod	Porphyromonas_A sp.	3.3	94.1	1.7	48.7	8557	1849389	Bacteria	Bacteroidota	Bacteroidia	Bacteroidales	Porphyromonadaceae	Porphyromonas_A	
MODERN	bin_17_mod	Prevotella sp.	6.4	99.3	0.5	49.3	57965	2990096	Bacteria	Bacteroidota	Bacteroidia	Bacteroidales	Bacteroidaceae	Prevotella	
MODERN	bin_42_mod	Prevotella sp	20.5	94.8	16.6	50.2	3512	4734899	Bacteria	Bacteroidota	Bacteroidia	Bacteroidales	Bacteroidaceae	Prevotella	
MODERN	bin_44_mod	Prevotella sp	1.3	51.0	3.4	52.7	1848	1855959	Bacteria	Bacteroidota	Bacteroidia	Bacteroidales	Bacteroidaceae	Prevotella	
MODERN	bin_8_mod	Prevotella sp	4.0	83.5	3.5	53.8	12697	2512812	Bacteria	Bacteroidota	Bacteroidia	Bacteroidales	Bacteroidaceae	Prevotella	
MODERN	bin_27_mod	Prevotella sp017627765	1.9	79.6	2.5	42.1	4848	2174706	Bacteria	Bacteroidota	Bacteroidia	Bacteroidales	Bacteroidaceae	Prevotella	Prevotella sp017627765

Co-Assembly batch	BIN	OTU	Sum abundance	Completion [%]	Contamination [%]	GC [%]	N50	Total length [bp]	domain	phylum	class	order	family	genus	species
MODERN	bin_31_mod	Prevotella sp905235835	3.5	61.8	1.9	47.8	3220	1699011	Bacteria	Bacteroidota	Bacteroidia	Bacteroidales	Bacteroidaceae	Prevotella	Prevotella sp905235835
ANCIENT	bin_E_dup	Propionibacterium ruminifibrarum	403.4	55.6	3.5	67.8	2769	1730795	Bacteria	Actinobacteriota	Actinomycetia	Propionibacteriales	Propionibacteriaceae	Propionibacterium	Propionibacterium sp900289195
MODERN	bin_E_dup	Propionibacterium ruminifibrarum	403.4	96.8	3.6	68.7	12018	2682438	Bacteria	Actinobacteriota	Actinomycetia	Propionibacteriales	Propionibacteriaceae	Propionibacterium	Propionibacterium sp900289195
MODERN	bin_2_mod	Proteiniphilum sp.	5.6	90.4	3.0	45.5	7248	3496335	Bacteria	Bacteroidota	Bacteroidia	Bacteroidales	Dysgonomonadaceae	Proteiniphilum	
ANCIENT	bin_39_anc	Pseudarthrobacter sp.	3.4	60.8	4.3	65.4	2460	2861831	Bacteria	Actinobacteriota	Actinomycetia	Actinomycetales	Micrococcaceae	Pseudarthrobacter	
ANCIENT	bin_37_anc	Pseudomonas_E lundensis	61.0	97.7	6.8	58.8	23369	4855647	Bacteria	Proteobacteria	Gammaproteobacteria	Pseudomonadales	Pseudomonadaceae	Pseudomonas_E	Pseudomonas_E lundensis
MODERN	bin_5_mod	Pseudomonas_E paraversuta	15.7	70.5	15.6	56.4	3152	980793	Bacteria	Proteobacteria	Gammaproteobacteria	Pseudomonadales	Pseudomonadaceae	Pseudomonas_E	Pseudomonas_E paraversuta
MODERN	bin_23_mod	Pseudomonas_E sp003014915	6.1	58.3	6.9	60.3	2515	7413950	Bacteria	Proteobacteria	Gammaproteobacteria	Pseudomonadales	Pseudomonadaceae	Pseudomonas_E	Pseudomonas_E sp003014915
MODERN	bin_41_mod	Psychrobacter sp.	8.7	89.9	2.9	42.8	6134	2879938	Bacteria	Proteobacteria	Gammaproteobacteria	Pseudomonadales	Moraxellaceae	Psychrobacter	
ANCIENT	bin_2	Rickettsia felis	8.8	81.4	1.3	32.9	3807	1160887	Bacteria	Proteobac	Alphaprot	Rickettsial	Rickettsia	Rickettsia	Rickettsia

Co-Assembly batch	BIN	OTU	Sum abundance	Completion [%]	Contamination [%]	GC [%]	N50	Total length [bp]	domain	phylum	class	order	family	genus	species
	6_anc									teria	eobacteria	es	ceae		felis
ANCIENT	bin_D_dup	RUG099 sp.	89.5	90.7	4.9	48.5	10083	2113659	Bacteria	Firmicutes_A	Clostridia	Peptostreptococcales	Anaerovoracaceae	RUG099	
MODERN	bin_D_dup	RUG099 sp.	89.5	69.2	4.8	48.4	3745	1692916	Bacteria	Firmicutes_A	Clostridia	Peptostreptococcales	Anaerovoracaceae	RUG099	
ANCIENT	bin_16_anc	RUG099 sp	16.3	61.5	3.4	46.2	3484	1081831	Bacteria	Firmicutes_A	Clostridia	Peptostreptococcales	Anaerovoracaceae	RUG099	
ANCIENT	bin_36_anc	RUG11795 sp.	122.7	68.0	2.0	39.5	3145	1667149	Bacteria	Firmicutes	Bacilli	Erysipelotrichales	Erysipelotrichaceae	RUG11795	
MODERN	bin_43_mod	RUG721 sp.	9.2	95.0	4.9	63.2	28527	2171499	Bacteria	Actinobacteriota	Coriobacteriia	Coriobacteriales	Atopobiaceae	RUG721	
MODERN	bin_37_mod	Saccharimonas sp.	9.0	63.7	0.4	48.2	129064	736272	Bacteria	Patescibacteria	Saccharimonadia	Saccharimonadales	Saccharimonadaceae	Saccharimonas	
ANCIENT	bin_55_anc	Saccharopolyspora dendranthemae	21.6	85.4	5.4	69.5	16887	5573339	Bacteria	Actinobacteriota	Actinomycetia	Mycobacteriales	Pseudonocardiaceae	Saccharopolyspora	Saccharopolyspora dendranthemae
ANCIENT	bin_24_anc	SFGY01 sp.	14.1	80.2	2.1	53.9	4358	1557077	Bacteria	Firmicutes_A	Clostridia	Saccharofermentanales	DTU023	SFGY01	
ANCIENT	bin_15_anc	Shewanella sp002966515	15.4	70.3	9.6	46.5	1939	4592395	Bacteria	Proteobacteria	Gammaproteobacteria	Enterobacterales	Shewanellaceae	Shewanella	Shewanella sp002966515

Co-Assembly batch	BIN	OTU	Sum abundance	Completion [%]	Contamination [%]	GC [%]	N50	Total length [bp]	domain	phylum	class	order	family	genus	species
ANCIENT	bin_59_anc	Staphylococcus equorum_A	7.7	85.0	10.9	32.4	3102	3331866	Bacteria	Firmicutes	Bacilli	Staphylococcales	Staphylococcaceae	Staphylococcus	Staphylococcus equorum_A
ANCIENT	bin_18_anc	Steroidobacter_A sp.	3.2	75.3	6.8	63	2830	4469609	Bacteria	Proteobacteria	Gammaproteobacteria	Steroidobacterales	Steroidobacteraceae	Steroidobacter_A	
ANCIENT	bin_14_anc	Steroidobacteraceae	6.0	94.4	5.9	65.5	22248	4692371	Bacteria	Proteobacteria	Gammaproteobacteria	Steroidobacterales	Steroidobacteraceae		
ANCIENT	bin_B_dup	Streptococcus chenjunshii	316.5	88.2	3.8	42.6	5709	2030032	Bacteria	Firmicutes	Bacilli	Lactobacillales	Streptococcaceae	Streptococcus	Streptococcus chenjunshii
MODERN	bin_B_dup	Streptococcus chenjunshii	316.5	95.1	0.2	41.6	27749	2162607	Bacteria	Firmicutes	Bacilli	Lactobacillales	Streptococcaceae	Streptococcus	Streptococcus chenjunshii
MODERN	bin_59_mod	Streptococcus gallolyticus	1.9	53.0	10.0	37.2	1490	1128409	Bacteria	Firmicutes	Bacilli	Lactobacillales	Streptococcaceae	Streptococcus	Streptococcus gallolyticus
ANCIENT	bin_56_anc	Streptococcus sp.	34.7	62.7	5.5	37.5	1774	1207602	Bacteria	Firmicutes	Bacilli	Lactobacillales	Streptococcaceae	Streptococcus	
ANCIENT	bin_40_anc	Streptomyces sp.	10.2	90.1	4.7	70.2	13783	5890215	Bacteria	Actinobacteriota	Actinomycetia	Streptomycetales	Streptomycetaceae	Streptomyces	
ANCIENT	bin_C_dup	Succiniclasticum sp.	86.9	94.6	3.9	46.9	7758	1694059	Bacteria	Firmicutes_C	Negativicutes	Acidaminococcales	Acidaminococcaceae	Succiniclasticum	
MODERN	bin_C_dup	Succiniclasticum sp.	86.9	95.6	2.0	46.7	29959	1989528	Bacteria	Firmicutes_C	Negativicutes	Acidaminococcales	Acidaminococcacea	Succiniclasticum	

Co-Assembly batch	BIN	OTU	Sum abundance	Completion [%]	Contamination [%]	GC [%]	N50	Total length [bp]	domain	phylum	class	order	family	genus	species
													e		
ANCIENT	bin_43_anc	SZUA-320 sp.	3.2	67.0	2.3	68	11686	3476177	Bacteria	Gemmatimonadota	Gemmatimonadetes	Gemmatimonadales	GWC2-71-9	SZUA-320	
MODERN	bin_39_mod	Treponema_D sp.	2.3	84.6	0.7	57.6	5425	2172720	Bacteria	Spirochaetota	Spirochaetia	Treponematales	Treponemataceae	Treponema_D	
MODERN	bin_52_mod	Treponema_D sp	2.1	72.7	0.7	48.5	3142	1660700	Bacteria	Spirochaetota	Spirochaetia	Treponematales	Treponemataceae	Treponema_D	
MODERN	bin_40_mod	UBA1066 sp.	1.9	53.8	3.1	58.6	1825	1339081	Bacteria	Firmicutes_A	Clostridia	Lachnospirales	Lachnospiraceae	UBA1066	
MODERN	bin_53_mod	UBA1367 sp.	3.0	75.8	1.5	62.7	4744	1769629	Bacteria	Actinobacteriota	Coriobacteriia	Coriobacteriales	Atopobiaceae	UBA1367	
ANCIENT	bin_25_anc	UBA1367 sp	17.9	56.6	4.1	66.4	2176	1664139	Bacteria	Actinobacteriota	Coriobacteriia	Coriobacteriales	Atopobiaceae	UBA1367	
MODERN	bin_19_mod	UBA2868 sp905235745	2.3	82.5	3.5	48.2	5319	1852118	Bacteria	Firmicutes_A	Clostridia	Lachnospirales	Lachnospiraceae	UBA2868	UBA2868 sp905235745
ANCIENT	bin_53_anc	UBA3738 sp.	26.7	84.2	5.0	45.1	6916	1475007	Bacteria	Firmicutes_A	Clostridia	Peptostreptococcales	Anaerovoracaceae	UBA3738	
ANCIENT	bin_13_anc	UBA4312 sp.	46.8	75.0	5.7	43.4	5127	1714447	Bacteria	Firmicutes	Bacilli	Erysipelotrichales	Erysipelotrichaceae	UBA4312	
MODERN	bin_13_mod	UBA4312 sp002394635	1.2	56.6	14.3	41.5	1614	1856396	Bacteria	Firmicutes	Bacilli	Erysipelotrichales	Erysipelotrichaceae	UBA4312	UBA4312 sp002394635

Co-Assembly batch	BIN	OTU	Sum abundance	Completion [%]	Contamination [%]	GC [%]	N50	Total length [bp]	domain	phylum	class	order	family	genus	species
ANCIENT	bin_17_anc	UBA7541	5.3	94.0	3.6	62	29026	4496507	Bacteria	Acidobacteriota	Acidobacteriae	Acidoferrales	UBA7541		
ANCIENT	bin_54_anc	UBA7541.1	2.1	60.5	2.1	63.9	3386	2247358	Bacteria	Acidobacteriota	Acidobacteriae	Acidoferrales	UBA7541		
ANCIENT	bin_30_anc	UBA9715 sp.	16.9	74.3	7.3	55.8	3258	2477898	Bacteria	Actinobacteriota	Coriobacteriia	Coriobacteriales	Eggerthellaceae	UBA9715	
ANCIENT	bin_7_anc	UBA9715 sp	51.1	72.8	2.5	60	6621	2432159	Bacteria	Actinobacteriota	Coriobacteriia	Coriobacteriales	Eggerthellaceae	UBA9715	
MODERN	bin_60_mod	W3P20-009 sp905235955	3.6	91.2	1.0	42.5	6419	2459179	Bacteria	Bacteroidota	Bacteroidia	Bacteroidales	W3P20-009	W3P20-009	W3P20-009 sp905235955
ANCIENT	bin_1_anc	WHSY01 sp.	75.3	97.8	6.0	70	14788	4179738	Bacteria	Actinobacteriota	Actinomycetia	Mycobacteriales	Pseudonocardiaceae	WHSY01	
ANCIENT	bin_5_anc	Yaniella sp.	8.9	95.2	1.2	56.5	179919	3329375	Bacteria	Actinobacteriota	Actinomycetia	Actinomycetales	Micrococcaceae	Yaniella	

Supplementary Table 2: Differential abundance of microbial taxa in 37 modern and ancient samples. Results are shown for associations with false-discovery-rate (FDR) < 0.05. MAGs with a positive coefficient (> 0) had higher abundance in the modern samples, while those with a negative coefficient (< 0) were more abundant in ancient samples. Blanks, historical samples and ancient samples U027, U035 and LB003 were excluded from the analysis. Values are rounded to three decimal places.

Bin	OTU	coefficient	standard error	p-value	FDR
bin_E_dup	Propionibacterium ruminifibrarum	-2.002	0.364	0	0
bin_D_dup	RUG099 sp.	-5.378	0.416	0	0
bin_C_dup	Succiniclasticum sp.	-1.384	0.418	0.002	0.004
bin_B_dup	Streptococcus chenjunshii	-4.263	0.43	0	0
bin_A_dup	Basfia_A sp.	1.965	0.725	0.01	0.016
bin_8_mod	Prevotella sp..3	1.069	0.317	0.002	0.003
bin_7_mod	JAGOWQ01 sp..1	3.613	0.337	0	0
bin_7_anc	UBA9715 sp..1	-3.754	0.358	0	0
bin_61_mod	Actinomyces sp. A.2	4.188	0.599	0	0
bin_6_anc	Amycolatopsis_C sp009377395	-0.855	0.323	0.012	0.018
bin_57_mod	Mannheimia sp..1	5.713	0.378	0	0
bin_57_anc	Lactobacillaceae	-0.788	0.243	0.003	0.004
bin_56_anc	Streptococcus sp.	-2.396	0.453	0	0
bin_55_anc	Saccharopolyspora dendranthemae	-2.705	0.463	0	0
bin_53_mod	UBA1367 sp.	1.33	0.362	0.001	0.002
bin_53_anc	UBA3738 sp.	-2.552	0.237	0	0
bin_50_mod	Fusobacterium_C necrophorum	0.548	0.213	0.015	0.02
bin_5_mod	Pseudomonas_E paraversuta	1.155	0.51	0.03	0.036
bin_49_mod	Bibersteinia sp.	1.197	0.478	0.017	0.023

Bin	OTU	coefficient	standard error	p-value	FDR
bin_48_anc	Allosaccharopolyspora sp..4	-0.917	0.352	0.013	0.019
bin_47_anc	Hornefia sp.	-1.987	0.285	0	0
bin_46_mod	Actinomyces sp. B	2.471	0.446	0	0
bin_45_mod	Bacteroides sp.	1.703	0.57	0.005	0.008
bin_45_anc	Bilifractor sp.	-1.981	0.168	0	0
bin_43_mod	RUG721 sp.	1.496	0.413	0.001	0.002
bin_41_anc	Methanobrevibacter_A sp..1	-0.927	0.382	0.021	0.027
bin_40_anc	Streptomyces sp.	-1.496	0.446	0.002	0.003
bin_4_mod	Neisseria sp.	1.875	0.537	0.001	0.003
bin_4_anc	Methanosphaera sp..1	-2.875	0.277	0	0
bin_38_anc	Methanobrevibacter sp.	-4.05	0.396	0	0
bin_36_anc	RUG11795 sp.	-2.178	0.112	0	0
bin_35_anc	Allosaccharopolyspora sp..3	-0.737	0.297	0.018	0.024
bin_34_mod	Peptidiphaga sp.	2.413	0.393	0	0
bin_33_anc	Methanobrevibacter_A sp.	-1.386	0.472	0.006	0.009
bin_32_mod	Actinomyces sp. A	0.836	0.347	0.022	0.027
bin_31_anc	CAG-791 sp.	-2.174	0.195	0	0
bin_30_anc	UBA9715 sp.	-1.352	0.349	0	0.001
bin_3_mod	Mannheimia sp.	0.741	0.304	0.02	0.026
bin_3_anc	Allosaccharopolyspora sp..2	-2.823	0.547	0	0
bin_29_mod	Cryptobacteroides sp.	1.961	0.499	0	0.001
bin_29_anc	Haemophilus_B sp.	-0.963	0.419	0.028	0.034
bin_28_anc	Methanosphaera sp.	-4.288	0.413	0	0

Bin	OTU	coefficient	standard error	p-value	FDR
bin_27_mod	Prevotella sp017627765	0.723	0.278	0.014	0.019
bin_26_mod	Porphyromonas_A sp.	0.666	0.293	0.029	0.036
bin_25_anc	UBA1367 sp..1	-2.025	0.338	0	0
bin_24_anc	SFGY01 sp.	-2.153	0.481	0	0
bin_23_anc	Allosaccharopolyspora sp..1	-1.429	0.395	0.001	0.002
bin_22_anc	Eubacterium_I sp..1	-2.134	0.31	0	0
bin_18_mod	Eubacterium_I sp.	1.752	0.439	0	0.001
bin_17_mod	Prevotella sp.	1.024	0.374	0.01	0.015
bin_16_anc	RUG099 sp..1	-1.455	0.387	0.001	0.001
bin_15_mod	Fusobacterium sp..1	1.307	0.404	0.003	0.005
bin_13_anc	UBA4312 sp.	-3.613	0.257	0	0
bin_12_mod	Desulfovibrio desulfuricans_D	2.043	0.309	0	0
bin_11_mod	Brachymonas sp.	2.434	0.407	0	0
bin_1_anc	WHSY01 sp.	-2.218	0.56	0	0.001

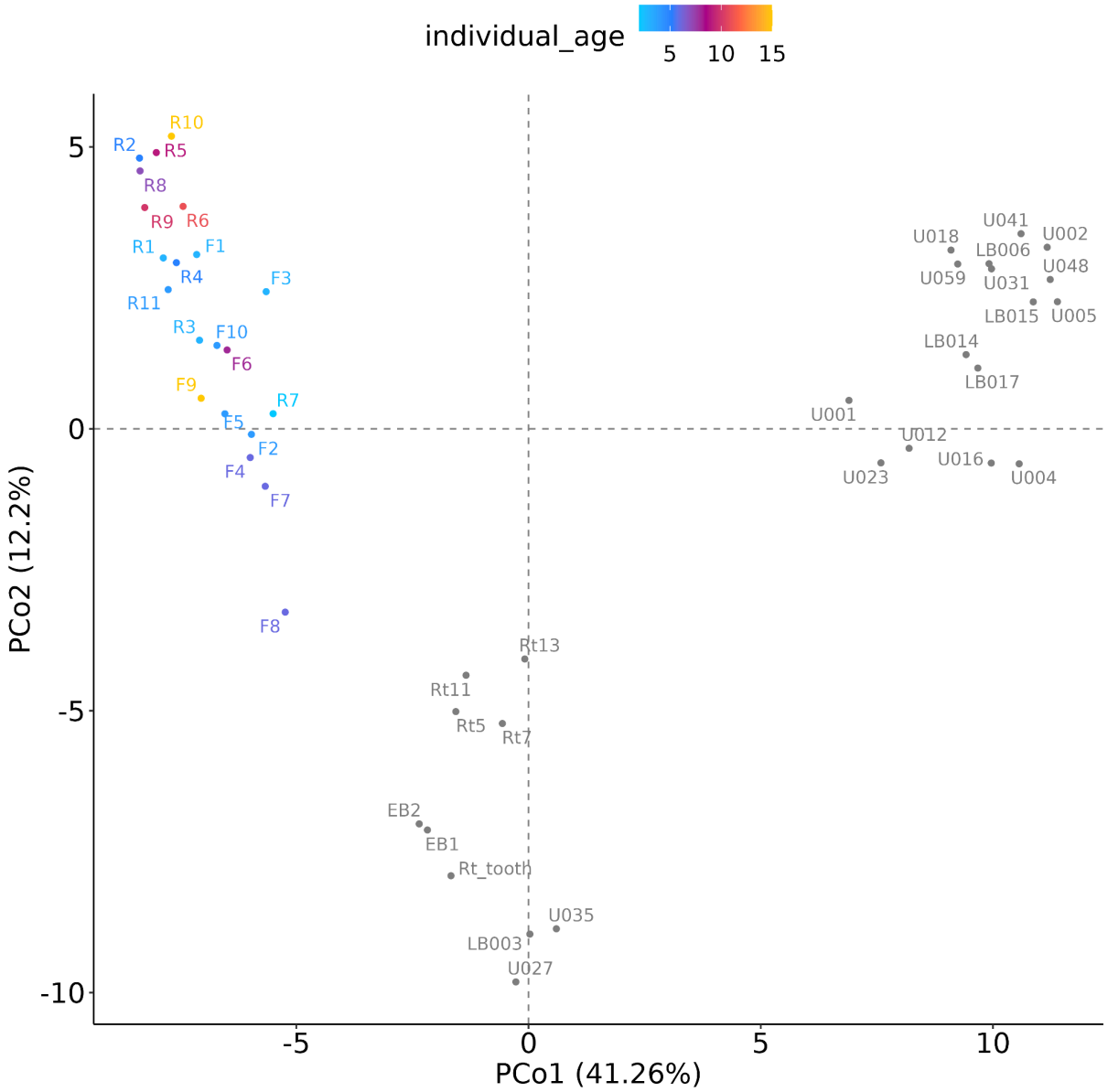

Supplementary Figure 1: PCoA plot of the relationship between taxon abundance, samples and individual age at death. Samples are colored by individual age at death (if known) on a scale from 2 to 15 years (see also table 1). Samples with unknown age at death and laboratory blanks are colored in gray. Abundance is corrected for detection threshold (considering samples to be 0 abundance if under detection limit.) Abundance values were log-transformed, with a pseudo-count of 0.001 for 0 abundance values (i.e. -3 after log-transformation). Samples with abundance equal to 0 are omitted.

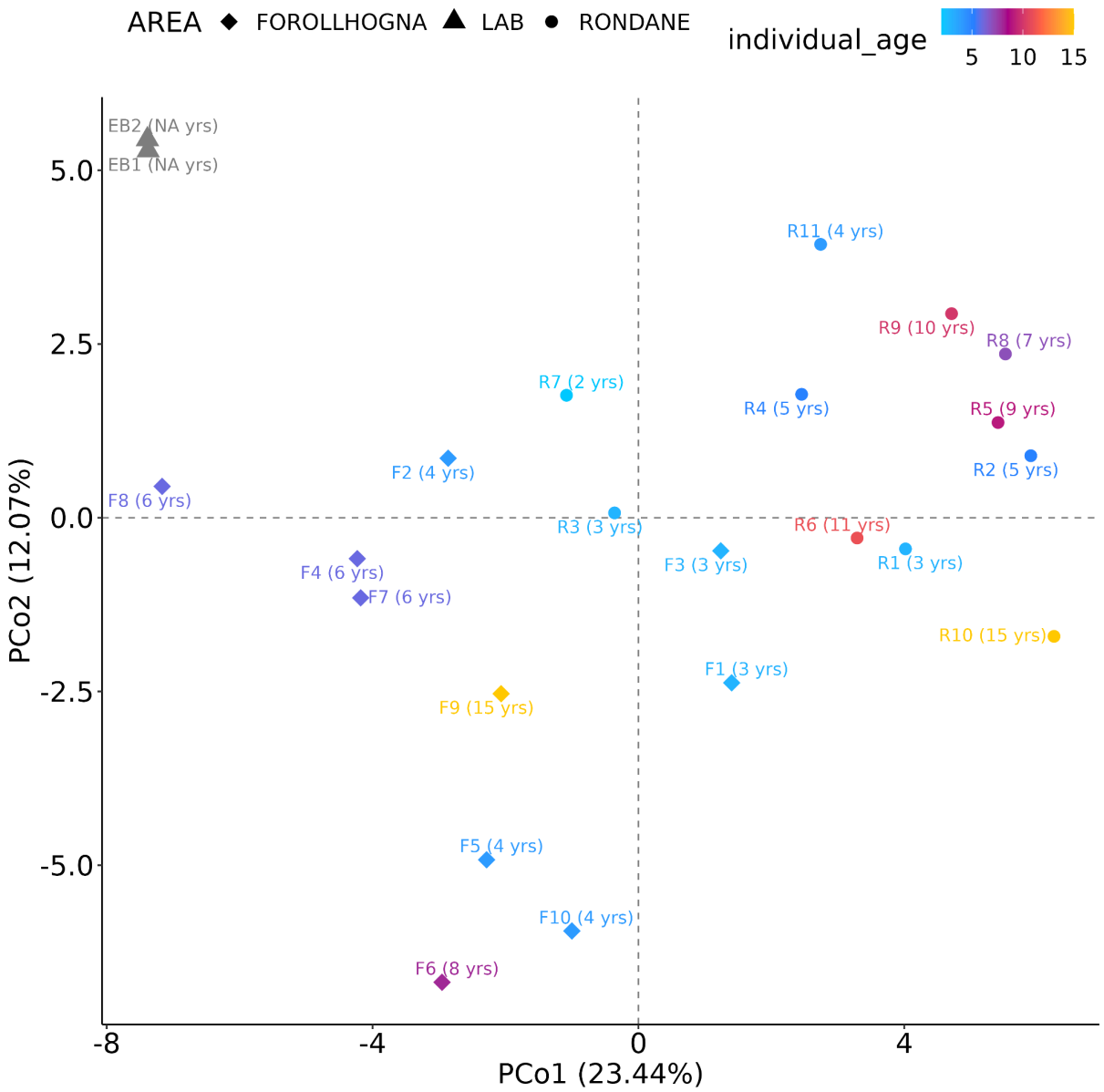

Supplementary Figure 2: PCoA plot of the relationship between taxon abundance, individual age at death and geography of modern samples. Ancient and historic samples were removed from the dataset for this analysis. Samples are colored by individual age at death on a scale from 2 to 15 years (see also table 1). Laboratory blanks are colored in gray. Geographic origin of samples is coded by shape (diamonds = Forollhogna, Norway; circles = Rondane, Norway; triangles = laboratory blanks). Each data point is labeled with sample name followed by individual age at death in parentheses. Abundance is corrected for detection threshold (considering samples to be 0 abundance if under detection limit.) Abundance values were log-transformed, with a pseudo-count of 0.001 for 0 abundance values (i.e. -3 after log-transformation). Samples with abundance equal to 0 are omitted.

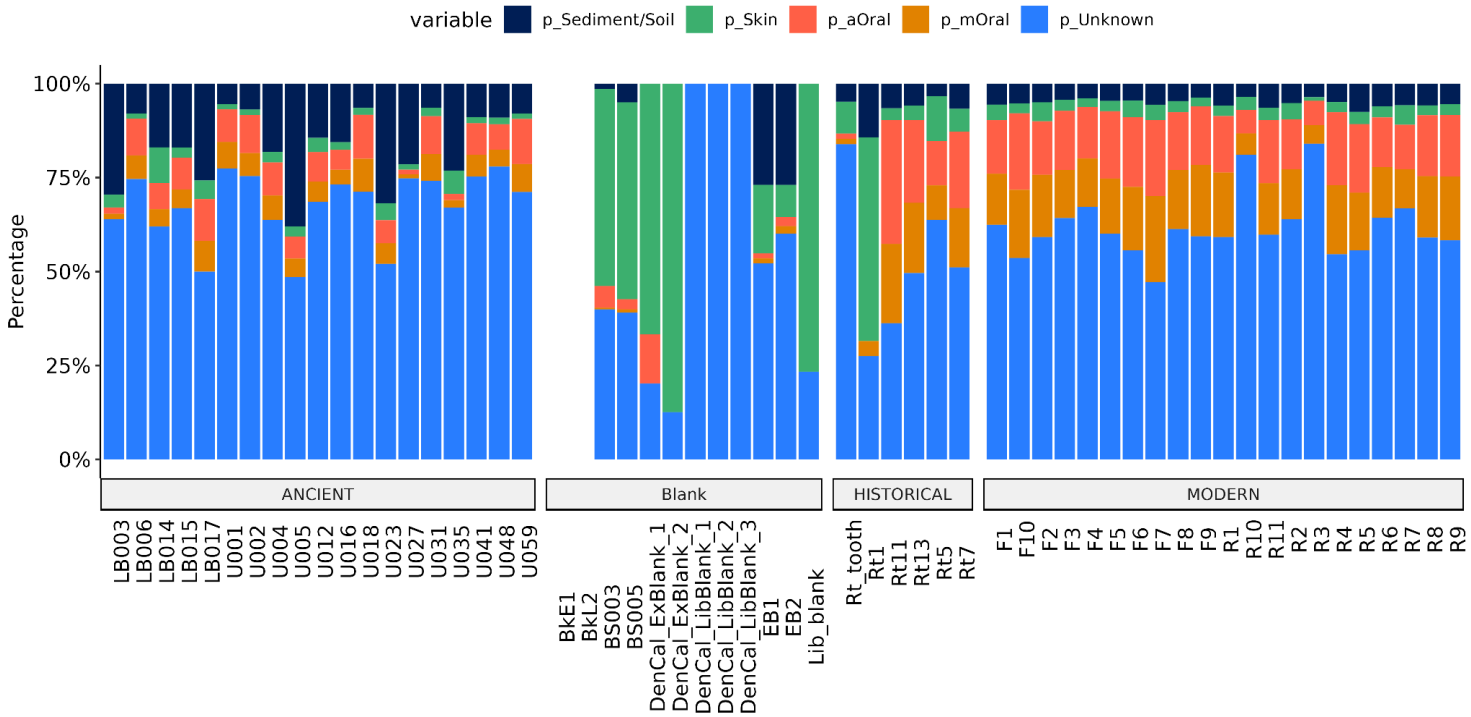

Supplementary Figure 3: Barplot of putative DNA source environments per sample. Samples are grouped by age. Classification was conducted with *decOM* (Duitama González et al. 2023) against the program's default database. aOral = ancient oral, mOral = modern oral.

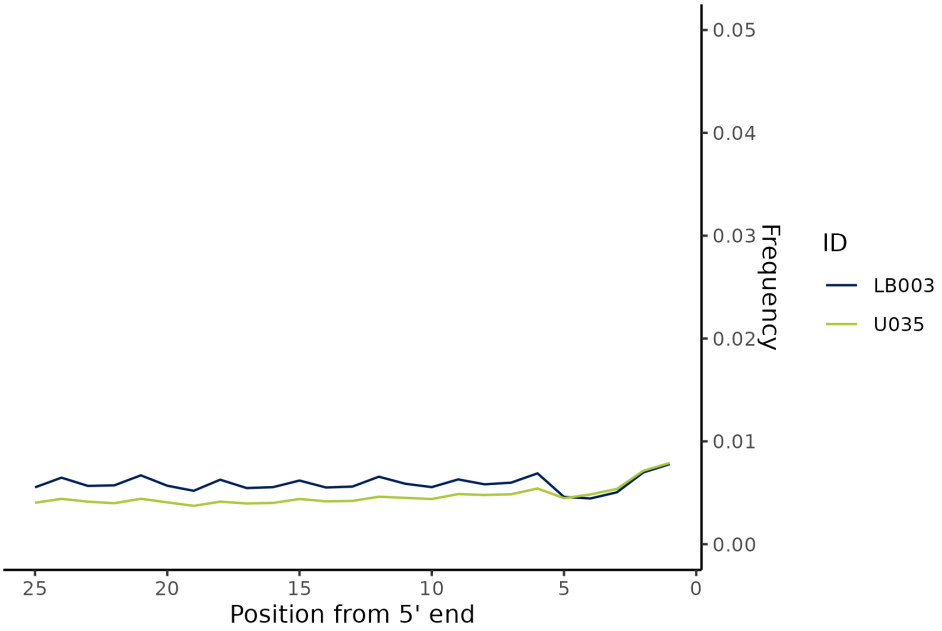

Supplementary Figure 4: Ancient DNA damage patterns for two samples with unusually low levels of damage. Frequency of cytosine-to-thymine transitions on the 5'-end of microbial reads have been calculated with *mapDamage2* (Jónsson et al. 2013).

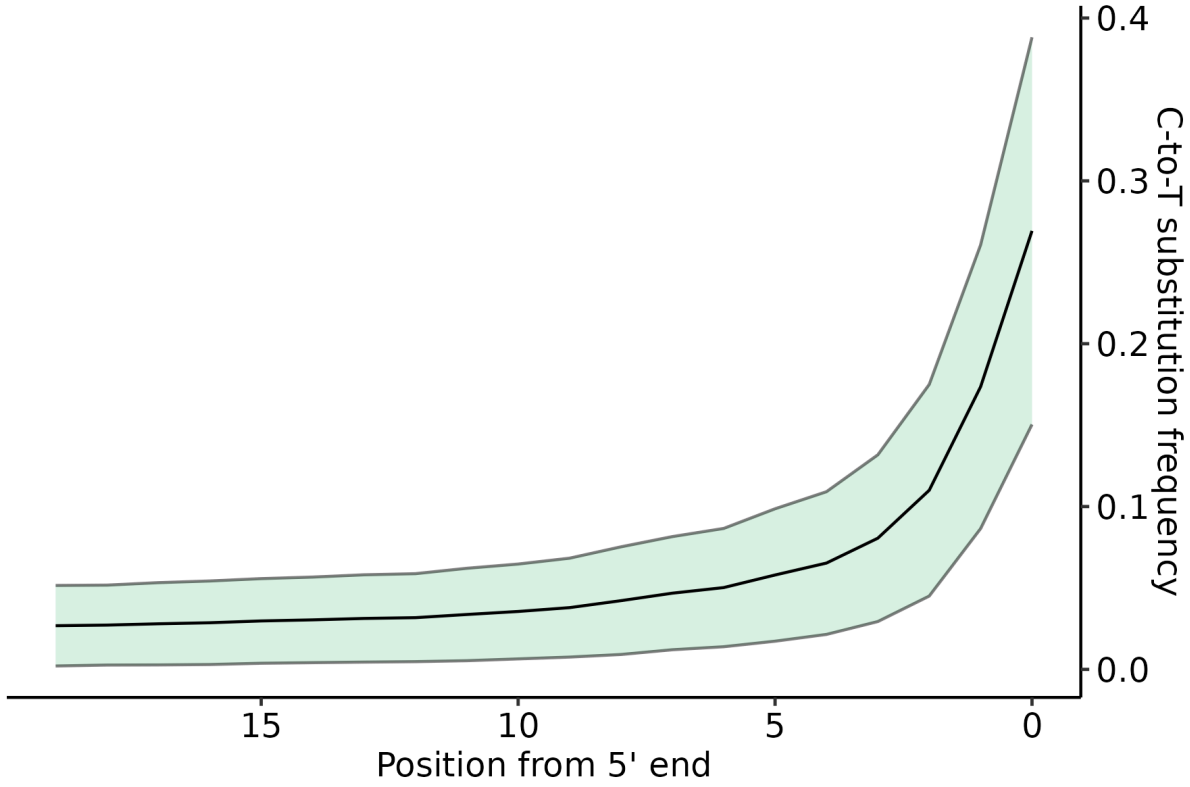

Supplementary Figure 5: Ancient DNA damage patterns in ancient samples. Frequency of cytosine-to-thymine transitions as estimated with *PyDamage* (Borry et al. 2021). Mean substitution frequency at each position from 5' end (black line). Gray lines bordering colored ribbon represent mean plus (upper) or minus (lower) one standard deviation.